FLORIDA STATE UNIVERSITY

COLLEGE OF ARTS AND SCIENCES

HEATWAVES IN FLORIDA AND THEIR FUTURE

By

PARKER ALEXANDER BEASLEY

A Thesis submitted to the
Department of Earth, Ocean, and Atmospheric Science
in partial fulfillment of the
requirements for the degree of
Master of Science

2023

Parker Beasley defended this thesis on March 30, 2023.
The members of the supervisory committee were:

Vasubandhu Misra
Professor Directing Thesis

Robert Hart
Committee Member

Jeffrey Chagnon
Committee Member

Rhys Parfitt
Committee Member

The Graduate School has verified and approved the above-named committee members and certifies that the thesis has been approved in accordance with university requirements.

I dedicate this thesis to my family: Lyle Beasley; Tracy Beasley; Heather Beasley; and Rita Wilkerson. My family has been an integral part of my academic success. I also want to dedicate this thesis to my girlfriend, friends back home, friends I have made during my time at Florida State University, and my professors.

ACKNOWLEDGMENTS

I acknowledge the support from NASA grants 80NSSC19K1199 and 80NSSC22K0595.

TABLE OF CONTENTS

LIST OF TABLES

LIST OF FIGURES

ABSTRACT

Florida, in the southeast US, is vulnerable to heatwaves due to its unique geolocation, exacerbated by both high temperature and humidity. To better understand the future impact on heatwave events over Florida we first conduct a retrospective analysis of these heat wave events in the current century using atmospheric reanalysis dataset (ERA5) as a verification dataset to verify two decades of simulations from a relatively high-resolution coupled ocean-atmosphere (RSM-ROMS) and atmosphere (RSM) only regional models. The analysis investigates the length, intensity, and characteristic kinematic and thermodynamic features of heatwave events over Florida between 1986-2005. After ascertaining the fidelity of the models from this retrospective analysis we proceeded to examine the future projection of the heatwave events for the decades of 2041-2060. The future projections are presented only for RSM since the differences from RSM-ROMS for the isolated heatwave events was found to be insignificant for the current and the future periods. We found the projected change of earlier first and later last dates of future heatwave events are associated with a projected increase in the mean surface temperature, a reduction of surface humidity, and a westward dislocation of the North Atlantic Subtropical High. Similarly, we also find that the frequency of the one, two, three, four, and five day heatwave events increase in the mid-21st century relative to the late-20th century period.

CHAPTER 1

INTRODUCTION

Florida has a unique climate compared to other states across the US because of its subtropical location, shape, and peninsular geography surrounded by relatively warm oceans. Since the state is exceptionally large, differences in climate occur between its northern and southern regions. Misra and Bhardwaj (2020) found that north and central Florida experience longer winters relative to south Florida, notably remarking that north Florida experiences the longest winter season in the state. Furthermore, they also found the opposite to be true for summer with south Florida experiencing a longer summer than north Florida. Another factor to highlight is the inter annual variability over Florida that occurs due to El Niño in the winter and spring seasons. El Niño events in the winter and spring are known to bring anomalous precipitation to Florida, resulting in a colder and wetter winter season (Hanson and Maul 1991). Contrastingly, El Niño events have far less influence over Florida's hydroclimate during the summer (Sittel 1994).

The state of Florida is prone to many types of extreme weather events that span across the year. For example, Hurricane season (1 June through 30 November) poses the highest potential for damage of all extreme weather events in Florida. Incidentally, Florida shares a large fraction of Atlantic landfalling tropical cyclones in the US (Knight and Davis 2009; Klotzbach et al. 2018). The National Oceanic and Atmospheric Administration's (NOAA) Office for Coastal Management recognizes the 2017 hurricane season with the highest recorded economic damage ever, totaling to more than $306 billion. It is estimated that Hurricane Irma, which made landfall in Florida, produced about $50 billion in damage. A study on Hurricane Irma found that all

vegetable crops in Florida experienced $180 million in damages and that citrus crops also took noticeable losses (Miller and Alvarez 2021).

Another example of extreme events in Florida is the vulnerability to coastal flooding. Wdowinski et al (2016) found the accelerated rate of sea level rise in southeast Florida to be 9 ± 4 mm/yr since 2006, a rate highly exceeding the global average of sea level rise, which makes the state more vulnerable to storm surges and high tides. Another extreme event that happens frequently in Florida is lightning. A study using storm data from NOAA from 1959-1994 found that Florida had the most deaths (345) and the most injuries (1178) from lightning during the time period (Curran et al. 2000). For the same period, the NWS recognizes 1523 reports of fatalities, injuries, and damage reports in Florida (https://www.weather.gov/cae/lightningdeaths.html).

It is not uncommon for regions of Florida to experience severe or even extreme droughts despite being surrounded by water bodies. Extreme or exceptional droughts are another threat that is most impactful during the driest season (boreal winter and spring) in Florida. Long durations of drought conditions are usually followed by wildfires that affect huge areas of the state (Thapa et al. 2013). However, unlike the southwest, long-term (decadal or longer) droughts are not prevalent in the southeastern US (Seager et al. 2009). But seasonal and monthly droughts are more common in southeastern US (Seager et al. 2009; Misra and Bastola 2016).

Furthermore, heatwaves occur in Florida, and are becoming more extreme and frequent in a warming climate (Perkins et al 2012). In Europe, there have been detrimental heatwave events

that have caused tens of thousands of deaths. The infamous European heatwave of 2003 was a result of localized forcings of sea surface temperature (SST) anomalies that impacted atmospheric circulation patterns (Fennessy and Kinter 2011). The research attributed local extreme SST anomalies as a key factor in altering the atmospheric state over southern and western European countries. Additionally, anthropogenic warming and a strong jet stream over the region were also found to be other influential factors for the European heatwave event of 2003 (Sánchez-Benítez et al 2022) that led to a death toll between 22,000 and 35,000 people (Fennessy and Kinter 2011). Similarly, across China there has been a significant increase in the number of heatwave events and annual heatwave days since the year 2000 (Li et al. 2021). Li et al (2021) suggest the increase in heatwave days and events is a result of warming from greenhouse gasses, changes in atmospheric circulation anomalies, and urbanization effects. In California, research on nineteen heat events spanning 3-15 days in duration impacted human health and hospitalized more than 11,000 people (Guirguis et al 2014). Health impacts in the central valley and coasts of California were a result of a 4.5°C to 9.1°C increase in temperature (Guirguis et al 2014).

In the US, The National Weather Service (NWS) recognizes heat as the leading cause of weather related deaths with nearly 200 occurrences in 2021 (https://www.weather.gov/hazstat/). Heatwaves may not pose the greatest threat in terms of collateral damage and are probably less expensive overall, but they have been proven to be fatal. A case-control study from the 1995 Chicago heatwave found that persons who had pre-existing medical conditions or were socially isolated and did not have air conditioning were at the greatest risk of death during the heatwave (Semenza et al. 1996). At least 700 people died in this event (Semenza et al. 1996). In other words, aging demography is more vulnerable to heatwaves than other populations. This puts

Florida, with its rapidly growing population of senior citizens (Florida Tax Watch 2022) in the cross-hairs of heatwave impact on human fatality. Semenza et al. (1996) also estimated that more than 50 percent of the deaths related to heat waves could have been prevented if air conditioning had been present. In Florida, most homes have air conditioning, but for those that don't, there is a clear indication of an increased risk of death during a heat wave event. This is especially true of the workers who work outdoors (e.g., in farming, landscaping, construction activities, etc.). Heat waves increase the ambient heat level of work environments and can cause heat stress which then increases the risk of occupational accidents and injuries (Rameezdeen and Elmualim 2017). One study indicates that among crop workers there is an increase in dehydration levels between pre-shift and post-shift periods while working during the summer months, leading to kidney issues later on in life for some (Mix et al. 2018).

Across Florida, pronounced changes in heatwave frequency have occurred throughout the state, most notably in southern Florida and along the I-4 corridor that expands from Tampa to the east of Orlando (Keellings and Waylen 2014). Some studies note that areas close to water bodies (e.g., Gulf of Mexico, Atlantic Ocean) have an increased probability of extremely high temperatures given water bodies can regulate daytime maximum and nighttime minimum diurnal temperatures and differences (Raghavendra et al. 2019; Behrens et al. 2019; Schär et al 2004). Therefore, Florida is vulnerable to heat waves from its relatively small diurnal variations in surface temperature. Marine heatwaves have shown a positive trend in increasing value throughout the entire region of Florida and are linked to a general increase in sea surface temperature (SST) (Androulidakis and Kourafalou 2022). Additionally, a study using a weather research model to dynamically downscale the Community Earth System Model on the future of

the eastern United States estimates an increase in heatwave frequency (Wu et al. 2014). Wu et al note that heatwaves in 2057-2059 will be 3.5-6.4 times more frequent than in 2002-2004, and mortality will be 7.5-19.0 times higher than in 2002-2004. A study on heat related illnesses resulting in a death or provision of medical services among Florida residents found that the highest mortality rates are observed in the panhandle or northern Florida, whereas the lowest mortality rates are in the southern counties (Harduar Morano et al. 2016). Harduar Morano et al (2016) also found that average summer temperatures are higher and more variable in northern Florida compared to other regions of the state. Furthermore, they also suggest that high rates of heat related illnesses in south central Florida are due to the large population of the outdoor workforce.

Heatwaves are becoming longer and more frequent across regions of Florida and raise a concern about the future climate (Cloutier et al. 2019). According to the Environmental Protection Agency (EPA; https://www.epa.gov/sites/default/files/2016-08/documents/climate-change-fl.pdf), Florida has warmed more than one degree Fahrenheit during the last century. This adds additional concern to the severity of future heat waves across Florida. According to David Zierden (personal communication, January 10th, 2023), the highest summer temperatures are often found in the panhandle of Florida, not in the peninsular region (Fig. 1). He also mentioned Florida has seen a greater change in overnight minimum temperatures rather than daytime highs. This is also reaffirmed in a study by Thomas et al (2020) that analyzed the North American warm season of June, July, and August for 1980-2018 daytime and nighttime surface temperatures. Thomas et al. (2020) found that mechanisms associated with nighttime heat waves differ by region. In the southeast, nighttime heatwave days are associated with anomalous low-

level southerly flow leading to warm air advection into the region. While Florida is not the only state in the southeast it has the largest amount of coastline. This gives room for nighttime warm air advection off of surrounding bodies of water. A potential increase in the frequency and intensity of heatwave events in future climate, therefore, underlines the importance of being able to understand these events and their changing characteristics (Sheridan and Lee 2018).

In this study, the focus is to understand the heatwave events from two unique 20-year integrations of a regional climate model centered over Florida for the current (1986-2005) and mid-21st century (2041-2060) climate. These regional climate model integrations were conducted at an unprecedented 10 km grid spacing with one of them coupled to a regional ocean model at the same 10 km grid spacing while the other is just the regional atmospheric model with prescribed SST from the driving global model. This resolution offers a reasonable depiction of the Geography of Florida that is otherwise poorly represented in global climate models that have grid resolutions usually > 100 km (Misra et al. 2019; Narotsky and Misra 2022).

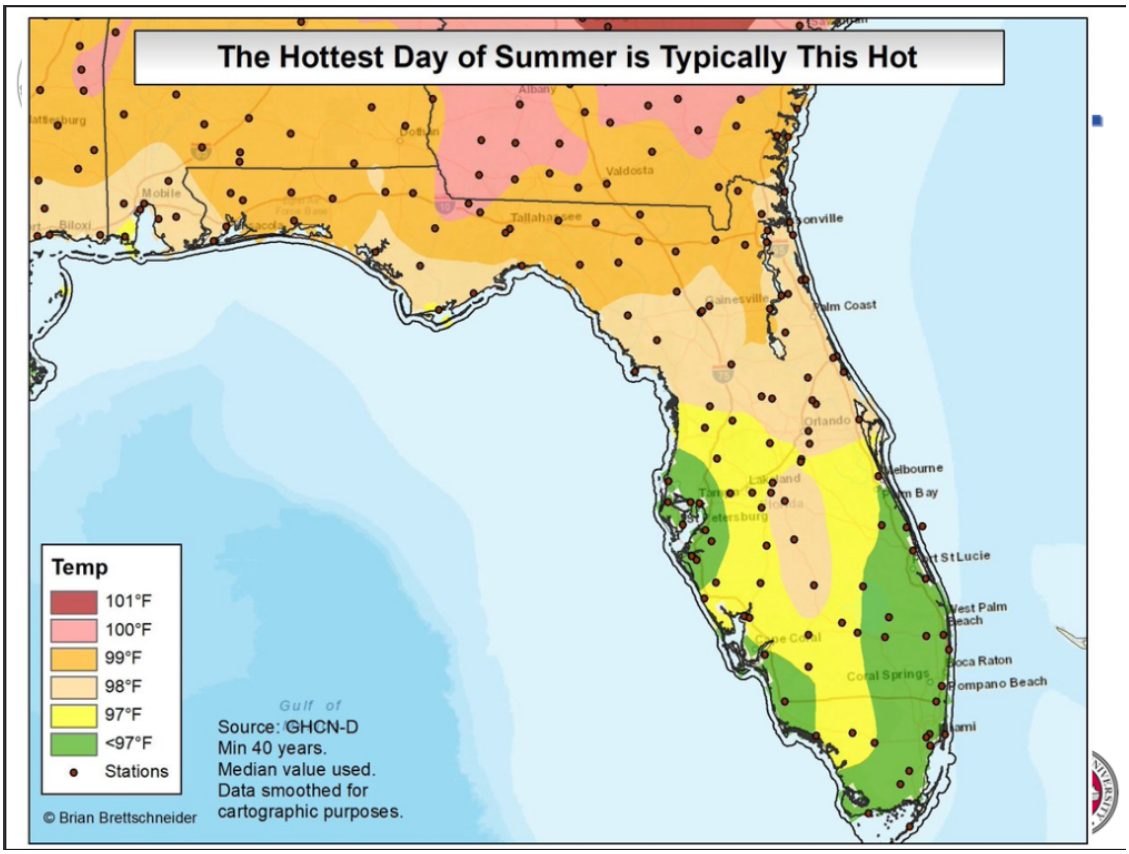

Fig. 1: The typical hottest day of Summer in Florida. From Brian Brettschneider, University of Alaska, Fairbanks, and NOAA.

CHAPTER 2

DATA

One of the objectives of this work is to analyze, verify, and compare two model integrations with their heat wave simulations against the corresponding reanalysis derived dataset. The other objective is to assess the future of heat wave events over Florida in the mid-21st century from these model integrations. The two modeled datasets are, (1) Regional Spectral Model (RSM) with prescribed SST and (2) RSM coupled to Regional Ocean Modeling System (ROMS) (Misra et al 2022). The verification data is from the reanalysis dataset provided by the European Center for Medium Range Weather Forecasts (ECMWF) Reanalysis version 5 (ERA5; Hersbach et al. 2019).

The Regional Spectral Model (RSM) Dataset

In this study, we are using the multiple decades of integration at 10km grid resolution of the Regional Spectral Model (RSM). The RSM was originally introduced by Juang and Kanamitsu (1994). Additional changes to the model follow those from Misra et al. (2019). The RSM downscales the atmospheric component of the climate system. Sea surface temperature (SST) is prescribed from the global coupled ocean–atmosphere model that forces it at the lateral boundaries. The RSM is a widely used model for climate studies (e.g., Misra et al. 2001; Roads 2004; He et al. 2015; Misra et al 2019). The dynamics of the RSM uses the spectral method, utilizing sine and cosine series to solve the primitive equations (Juang and Kanamitsu 1994). Additionally, the RSM uses a spectral damping scheme for the reduction of climate drift and also allows for nesting ratios that are larger than what is traditionally used (Kanamaru and Kanamitsu 2007). The vertical coordinate system uses a terrain following 28 sigma levels where the top of

the atmosphere is fixed at ~ 2hPa. The RSM integration used in this study is forced at the lateral boundaries by the atmospheric variables and at the surface by the SST from the Community Climate System Model version 4 (CCSM4; Gent et al. 2011) simulation for the current (1986-2005) and the future (2041-2060) climate periods. These integrations have been analyzed for their hydroclimatic variations and change over Florida and in the surrounding oceans in great detail in Misra and Bhardwaj (2022).

The Regional Spectral Model-Regional Ocean Model System (RSM-ROMS) Dataset

This study also utilizes multiple decades of integration of the Regional Spectral Model-Regional Ocean Model System (RSM-ROMS), which is the coupled version of the RSM. The ocean component of RSM-ROMS is based on the Regional Ocean Modeling System (ROMS; Haidvogel et al. 2000; Shchepetkin and McWilliams 2005). No flux corrections are applied during the integration of RSM-ROMS. The components of RSM-ROMS are integrated using identical discretization of grids for RSM and ROMS at 10 km grid spacing. Several studies have examined the fidelity of the RSM and RSM-ROMS integrations analyzed for this study (Bhardwaj and Misra 2019; Misra et al. 2019; Misra and Bhardwaj 2021; Misra and Bhardwaj 2022). We will use two 20-year periods to represent the current (1986-2005) and the future (2041-2060 or the mid-21st century) climate over the regional domain centered over Florida from both RSM and RSM-ROMS.

The lateral and initial boundary conditions for RSM-ROMS for present and future climate simulations were from the oceanic and the atmospheric components of the Community Climate System Model version 4 (CCSM4) simulation and are linearly interpolated to the

corresponding grids (Misra et al. 2019). The RSM and ROMS are forced at 6-hour and monthly intervals at the lateral boundaries, respectively.

Misra et al. (2019) indicate that the RSM-ROMS integration for the period 1986-2005 centered over peninsular Florida shows considerable improvement over the parent global model CCSM4. For example, the upper ocean thermal stratification, representation of the surface eddy kinetic energy of the ocean and the Loop Current, and terrestrial rainfall over Peninsular Florida are significantly improved in RSM-ROMS compared to CCSM4. They attribute some of these improvements to the improvement in the ocean bathymetry at 10 km grid resolution of the RSM-ROMS relative to ~ 1° grid spacing of CCSM4 ocean. The resulting improvement in the neighboring oceans then results in an impact on the terrestrial rainfall over Peninsular Florida from changes in the mean horizontal gradients of moisture and divergence of atmospheric moisture flux (Misra and Bhardwaj 2022). Bhardwaj and Misra (2019) found that RSM-ROMS has a lower systematic error of seasonal mean precipitation, surface evaporation, and moisture flux convergence over WFS and peninsular Florida compared to the corresponding RSM integration.

The ERA5 Dataset

The ERA5 dataset is available on a 31km grid and spans 137 levels from the surface to a height of 80km (ECMWF). The data is archived in the ECMWF data archive, MARS, and a pertinent subset of the data that is interpolated to a regular latitude/longitude grid was copied to the C3S Climate Data Store (CDS) disks (https://confluence.ecmwf.int/display/CKB/ERA5%3A+data+documentation). Data in an hourly

format is readily available and dates back to 1959. However, in this work, we analyzed daily averages at the surface from 1986 to 2005 to coincide with the model integration.

ERA5 dataset has been widely used for heat wave studies (Liu et al. 2020; Li 2020; Mukherjee and Mishra 2020; Zhang et al. 2021). Russo and Domeisen (2022) show that ERA5 daily maximum temperatures display significant fidelity when verified with other independent observation datasets on a global scale. However, for different reanalysis datasets, it has been shown that there are inconsistencies between them when analyzing heatwaves across the US (Schoof et al 2017). Schoof et al. (2017) note that the four reanalyses (ERA-Interim, JRA-55, MERRA-2, and NARR) agreed on the sign of the regional trend for heatwaves but differed on the magnitude and statistical significance for the northwest, southeast and southern planes regions of the US.

CHAPTER 3

METHODOLOGY

A universal definition of heat waves does not exist. Perkins et al. (2012) mention that heatwaves are loosely defined as a period of singular or consecutive days where conditions are hotter than normal. Whereas the National Weather Service (NWS) defines a heatwave as a period of abnormally hot weather lasting more than two days and can occur with or without high humidity. In this study, equation (1) is used to evaluate the heat index.

$$I_{NWS} = -42.379 + 2.04901523\mathrm{T} + 10.14333127\mathrm{R} - 0.22475541\mathrm{TR} - 0.00683783\mathrm{T2} - 0.05481717\mathrm{R2} + 0.00122874\mathrm{T2R} + 0.00085282\mathrm{T2R2} - 0.00000199\mathrm{T2R2} \quad -----(1)$$

Where, I_{NWS}, T, and R represent heat index in °F, the temperature in °F and relative humidity in percentage. I_{NWS} is calculated each hour throughout the day and the daily maximum I_{NWS} is classified into one of four categories HI13 through HI16 (Table 1). An adjustment to I_{NWS} (I_{NWS}^{*}) computed from Equation 1 is made when R is less than 13% and T is between 80°F and 112°F as:

$$I_{NWS}^{*} = I_{NWS} - B \quad ----------(2)$$

Where,

$$B = \frac{(13 - R)}{4}\sqrt{\frac{17 - |T - 95|}{17}} \quad ----------(3)$$

However, if R is greater than 85% and T is greater than 80°F but less than 87°F then B takes the form:

$$B = \frac{(R - 85)}{10} \times \frac{(87 - T)}{5} \quad ----------(4)$$

The adjustments made to I_{NWS} (I_{NWS}^{*}) are applied to compute a maximum heat index using the Weather Prediction Center (WPC) or Model Output Statistics (MOS) forecast maximum temperature and the 00 UTC dewpoint temperature at each forecast grid point for each day (https://www.wpc.ncep.noaa.gov/heat_index/details_hi.html). Equation (1) is a regression computed by Lans. P Rothfusz, and is not appropriate for use when temperature and humidity conditions don't warrant a heat index value below 80°F, and is not valid for extreme cases of temperature and relative humidity beyond specific ranges of values (https://www.wpc.ncep.noaa.gov/heat_index/details_hi.html). Table (2) was created by the NWS and depicts heat index values based on Equation (1) and the adjustments in Equations (3) and (4).

The RSM and RSM-ROMS integrations store the prognostic variables of daily mean humidity and temperature, which is used for calculating I_{NWS} and or I_{NWS}^{*}. Upon computing daily values of I_{NWS} we use Table (1) following Smith et al. (2013) to define HI13 when I_{NWS} exceeds 80°F. We then follow by identifying the first and last day of the occurrence of HI13 each year for the current and future climate from the two model integrations and ERA5. We also computed the frequency of the duration of the 1-day, 2-day, 3-day, 4-day, and 5-day heat wave events for each year from all three datasets.

We have also created composites of humidity, temperature, and 850hPa circulation fields for these various heatwave events to characterize them in greater detail and understand the change in a future mid-21st century climate.

Table 1 - Definitions of heat wave indices. Reproduced from Smith et al. (2013)

Heatwave index	Temperature metric	Threshold	Duration	Type	Reference
HI01	Mean daily temperature	➢ 95th percentile	2+ consecutive days	Relative	Anderson and Bell (2011)
HI02	Mean daily temperature	➢ 90th percentile	2+ consecutive days	Relative	Anderson and Bell (2011
HI03	Mean daily temperature	➢ 98th percentile	2+ consecutive days	Relative	Anderson and Bell (2011
HI04	Mean daily temperature	➢ 99th percentile	2+ consecutive days	Relative	Anderson and Bell (2011
HI05	Minimum daily temperature	➢ 95th percentile	2+ consecutive days	Relative	Anderson and Bell (2011
HI06	Maximum daily temperature	➢ 95th percentile	2+ consecutive days	Relative	Anderson and Bell (2011
HI07	Maximum daily temperature	T1 > 81st percentile T2 > 97.5th percentile	1. Everyday > T1 2. 3+ consecutive days > T2 3. Avg Tmax > T1 for the whole time period	Relative	Peng et al. (2011); Meehl and Tebaldi (2004)
HI08	Maximum daily apparent temperature*	➢ 85th percentile	1 day	Relative	Steadman (1984)
HI09	Maximum daily apparent temperature*	➢ 90th percentile	1 day	Relative	Steadman (1984)
HI10	Maximum daily apparent temperature*	➢ 95th percentile	1 day	Relative	Steadman (1984)
HI11	Maximum daily temperature	➢ 35°C	1 day	Absolute	Tan et al. (2007)
HI12	Minimum and Maximum daily temperature	Tmin ≥26.7°C Tmax ≥40.6°C	At least one of the thresholds to be met for 2+ consecutive days	Absolute	Robinson (2001)
HI13^{+}	Maximum daily heat index	➢ 80°F	1 day	Absolute	NWS; Rothfusz and Scientific Services Division (1990); Steadman (1979)
HI14^{+}	Maximum daily heat index	➢ 90°F	1 day	Absolute	NWS; Rothfusz and Scientific Services Division (1990); Steadman (1979)
HI15^{+}	Maximum daily heat index	➢ 105°F	1 day	Absolute	NWS; Rothfusz and Scientific Services Division

					(1990); Steadman (1979)
HI16[+]	Maximum daily heat index	➢ 130°F	1 day	Absolute	NWS; Rothfusz and Scientific Services Division (1990); Steadman (1979)

*Apparent temperature in °C=-1.8+1.07T +2.4VP-0.92v +0.0444Q_g; where T is in °C, VP is vapor pressure in kPa, v is wind speed in ms^{-1}, Q_g is net extra radiation per unit area of the body surface in Wm^{-2}
+ Uses the INWS index provided in Equation 1 in the text.

Table 2 - Heat Index Values. From The National Weather Service from the National Oceanic and Atmospheric Administration. US Department of Commerce.

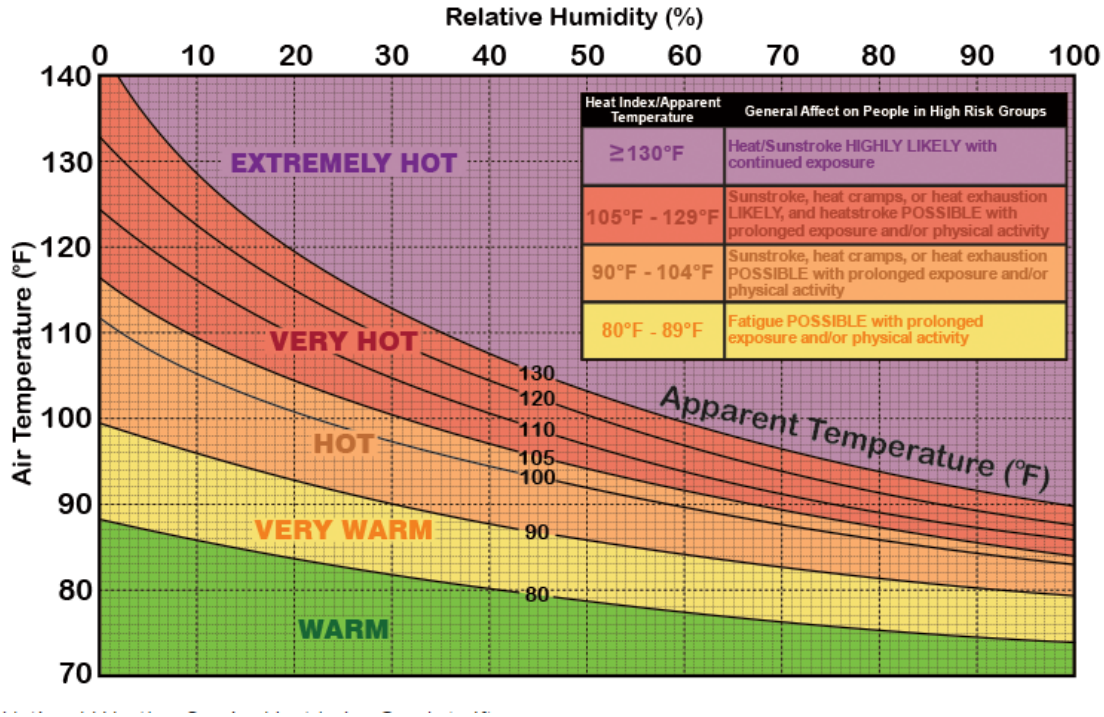

CHAPTER 4

RESULTS

Verification of URSM and CRSM late 20th-century simulations

As mentioned earlier, both URSM and CRSM have been extensively verified in earlier studies (e.g., Bhardwaj and Misra 2019; Misra et al. 2019; Misra and Bhardwaj 2021; Misra and Bhardwaj 2022). However, in this study, we specifically verify the heatwave simulation of the late 20th-century integration of URSM and CRSM forced by CCSM4 with the corresponding heatwave rendition in ERA5. The climatological distribution of the total number of 1-day heatwave events across Florida is shown in Fig. 2. The ERA5 reanalysis dataset shows a maximum in the number of 1-day heatwave events for south Florida, and a decrease in the total number of 1-day heatwave days with increasing latitude (Fig. 2a). In comparison, the uncoupled (URSM; Fig. 2b) and coupled (CRSM; Fig. 2c) models reasonably simulate the 1-day heatwave events, showing similar meridional gradient with a maximum in south Florida. However, the differences between URSM and CRSM are negligible (Fig. 2d). Furthermore, both models overestimate 1-day heatwave events for all regions of Florida (Figs. 2e and 2f). Similarly, Figs. 3-6 indicate a decrease in the total number of heatwave events. Furthermore, the frequency of longer heat wave events (2-5 day) is less than the shorter heat wave events. For example, 5-day events (Fig. 6) occur less often than 1-day events (Fig. 2). In addition, Fig. 3 shows that 2-day heatwave events occur less often than 1-day heatwave events. There is a recession of heatwave events, to the north, indicating a decrease in the total amount of heatwave events as latitude increases. Similarities are seen in Fig. 4 where there are less heatwave events for 3-day instances. The trend for a northward recession and decline in total number of heatwave events continues for 4-day (Fig. 5) and 5-day (Fig. 6) heatwave events.

The first day of the year when the 1-day heat wave event occurs for the ERA5 reanalysis dataset is fairly early in the year over south Florida around Julian day 100 or April 10, and is gradually delayed as you move further north to around Julian day 150 or May 30 over north Florida (Fig. 7a). The differences between URSM and CRSM for the first day of the heatwave event is insignificant (Fig. 7d). But both models simulate the first day of the heatwave in the year almost a month later than ERA5 over south Florida while in other parts of Florida, the simulation is reasonable (Figs. 7e and 7f).

The same can be said for the last day of the year for heatwaves, extending late into the year (Fig. 8a). The models also have the last 1-day heatwave event later in the year than the reanalysis dataset (Fig 8b and 8c).

In relation to the surface relative humidity for ERA5 (Fig. 9c), URSM20 underestimates surface relative humidity across Florida ranging from 4% to over 20% (Fig. 9d). Similar results are seen for other durations of heat wave events, 2-5-day (not shown). The 2 m air temperature underlies the systematic error from URSM20, suggesting a similar warm bias with respect to ERA5 (Fig. 10c and d). The specific humidity for URSM20 ranges from 13g/kg to over 18g/kg (Fig. 11a). This is an underestimation in relation to ERA5 (Figs. 11c and d) by about 3g/kg across Florida. For the 850hPa circulation, URSM20 underestimates the strength of the North Atlantic Subtropical High (NASH) relative to ERA5 (Fig. 12c) and displaces it further west than the latter.

While the models, URSM and CRSM, are mostly in agreement with the reanalysis dataset, they are in closer agreement with each other – in these heatwave metrics. Therefore, we choose to show the projections of the heatwave events from the mid-21st century simulation and further verification of the 20th-century simulations from only URSM.

Projections of the mid-21st century climate

Many studies suggest an increase in the frequency and amplitude of heatwaves over Florida in a future warming climate, which will potentially impact the elderly population and the outdoor workforce adversely (Keellings and Waylen 2014; Morano et al. 2016; Cloutier et al. 2019; Androulidakis and Kourafalou 2022).

Figs. 13a and b show the climatological first day of the heatwave in the late 20th and mid-21st century simulations of URSM and their corresponding difference in Fig. 13c. In this figure, we see that the climatological first day of the heatwave of the year – from URSM20, occurs around Julian day 140 across Florida. In contrast, URSM21 shows that in the mid-21st century the first day of the heatwave occurs around Julian day 110 (Figs. 13b and c), which is almost a month earlier compared to URSM20 (Fig. 13a). The differences between the two periods decrease slightly as you move further north over the panhandle Florida. The mid-21st century projection indicates the first presence of a heatwave event about a month earlier compared to the present model for the northern gulf coast and southern regions of Florida, and about 10-20 days earlier for central and northern regions of Florida compared to the 20th-century simulation (Fig. 13c).

Figs. 14a and b show comparisons of the climatological last day of the heatwave event for the year for both the present and future simulations, respectively. URSM20 suggests the last day of the 1-day heatwave event occurring in the year to be around Julian day 270 (Fig. 14a), whereas URSM21 projects the last day to be around Julian day 290. Fig. 14c shows the differences between the two models, suggesting a delay of the last day of occurrence of heatwaves in the year to be in the range of 5 to 25 days across, with the largest delays in south Florida and the northern Gulf coast. However, in the central and northern regions of Florida, differences of only 5-15 days are seen (Fig. 14c). This means the northern gulf coast and southern regions will, on average, experience 1-day heatwave events that occur earlier in the year and extend later into the year in a future climate. In terms of multiday events (2-5 days), the same pattern occurs where the future model predicts an earlier Julian date for the first occurrence in the year, and a later Julian date where the last occurrence happens (not shown).

The number of multi-day heatwave events that occur in URSM21 outnumbers the number of multi-day heatwave events in URSM20. Figs. 15b and 16b show the ratios of 2 to 5-day heat wave events to 1-day heat wave events. The higher the ratio, the higher correspondence and the more likely a multi-day event would occur if a 1-day event occurred. For instance, Fig, 15c shows the ratio of 3-day events to 1-day events from URSM20. This figure suggests that there is a high likelihood of 3-day events to occur if a 1-day event occurs over South Florida, but over north Florida, the ratio falls off and is, therefore, less likely to occur by about 10%. So, out of all days where our definition of a heatwave occurs, a 3-day event occurs ~80% of the time in south Florida, and only ~70% of the time in North Florida. The more days that occur in the event, the lower the percentage. A 5-day event occurs only ~50% of the time after a 1-day event over north

Florida and anywhere from 70-90% of the time for regions of south Florida (Fig. 15e). We see higher ratios along coastal regions. The biggest difference between URSM20 and URSM21 is that the percentages increase drastically with an increase in the number of heatwave days occurring successively. For example, Fig. 16 shows that nearly all heatwave events are at least 70% likely to occur in a future climate (2-5 day events).

To further examine these changes, we also analyzed the projected changes to the input variables used to compute the heat index that defines the heat waves (Equation 1). The climatological surface relative humidity associated with the 1-day heatwave event in the late 20th century in URSM20 (Fig. 9a) and in the mid-21st century climate in URSM21 (Fig. 9b) are very similar to each other (Fig. 9e). As mentioned earlier, URSM20 underestimates surface relative humidity across Florida ranging from 4% to over 20% (Fig. 9d) in comparison to ERA5 (9c).

In Figs. 10a and b, we show the climatological late 20th century and mid-21st century 2 m air temperature from URSM20 and URSM21 associated with the 1-day heatwave events, respectively. It is apparent from their comparison that the future climate suggests warming, ranging from 1 to 2°C (Fig. 10e). Expressed before, the systematic error from URSM20 suggests a similar warm bias with respect to ERA5 (Fig. 10c and d). Equation 1 from the Methodology Section tells us that if the temperature increases, while the relative humidity remains the same, then an overall increase in heat index occurs. For all heat wave events (1–5-day heat waves), the temperature increases by at least 1°C, and the relative humidity remains unchanged for the overwhelming majority of Florida (not shown). This accounts for part of the reason we see an increase in heat indices in a future climate over Florida.

Similarly, the 2 m specific humidity associated with 1-day heatwave event is shown from the model simulations and ERA5 in Fig. 11. As a reminder, the specific humidity for URSM20 is underestimated in relation to ERA5 (Figs. 11c and d). In contrast, in the mid-21st century URSM21 further increases the specific humidity ranging from 14g/kg to over 18g/kg (Figs. 11b and e). Close similarities are seen in the 2-day heatwave event simulations (not shown).

Additionally, we also examined the large-scale circulation at 850hPa associated with 1-day heatwave events (Fig. 12). The anticyclonic circulation of the NASH is apparent from the model simulations (Figs. 12a and b) and ERA5 (Fig. 16c). URSM20 underestimates the NASH relative to ERA5 (Fig. 12c), rendering it further west than ERA5. URSM21 in the mid-21st century suggests a slight weakening of NASH and the easterly trades relative to the late 20th-century simulation of URSM20 (Fig. 12e).

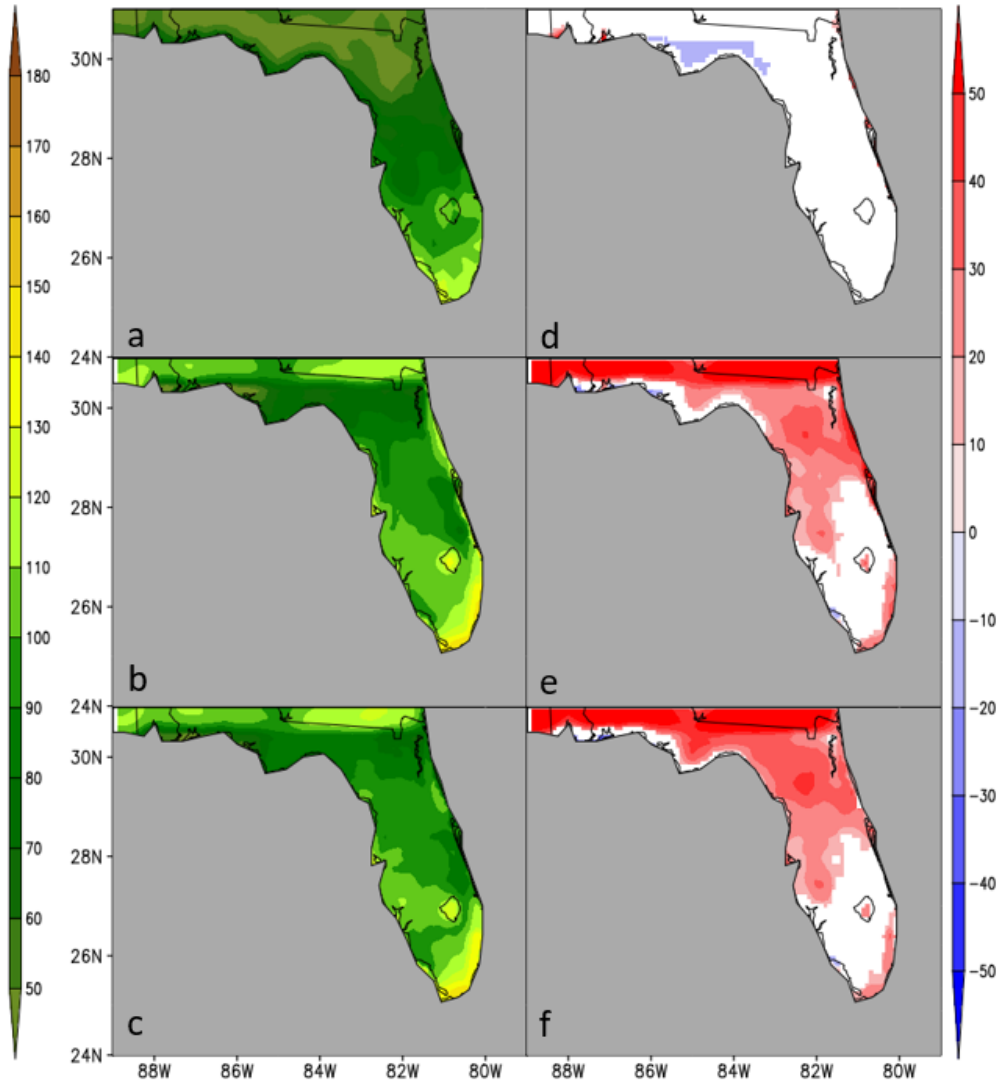

Fig. 2: The climatological number of 1-day heatwave events (heat index 80+ °F) over Florida for 1986-2005 (a) ERA5, (b) URSM, (c) CRSM, and (d) c-b. The corresponding systematic errors of (e) URSM and (f) CRSM. The difference between model (d) URSM-CRSM and corresponding systematic errors of (e) URSM, (f) CRSM. The differences which are statistically significant at 95% confidence interval according to t-test are shaded values in panels d, e, and f.

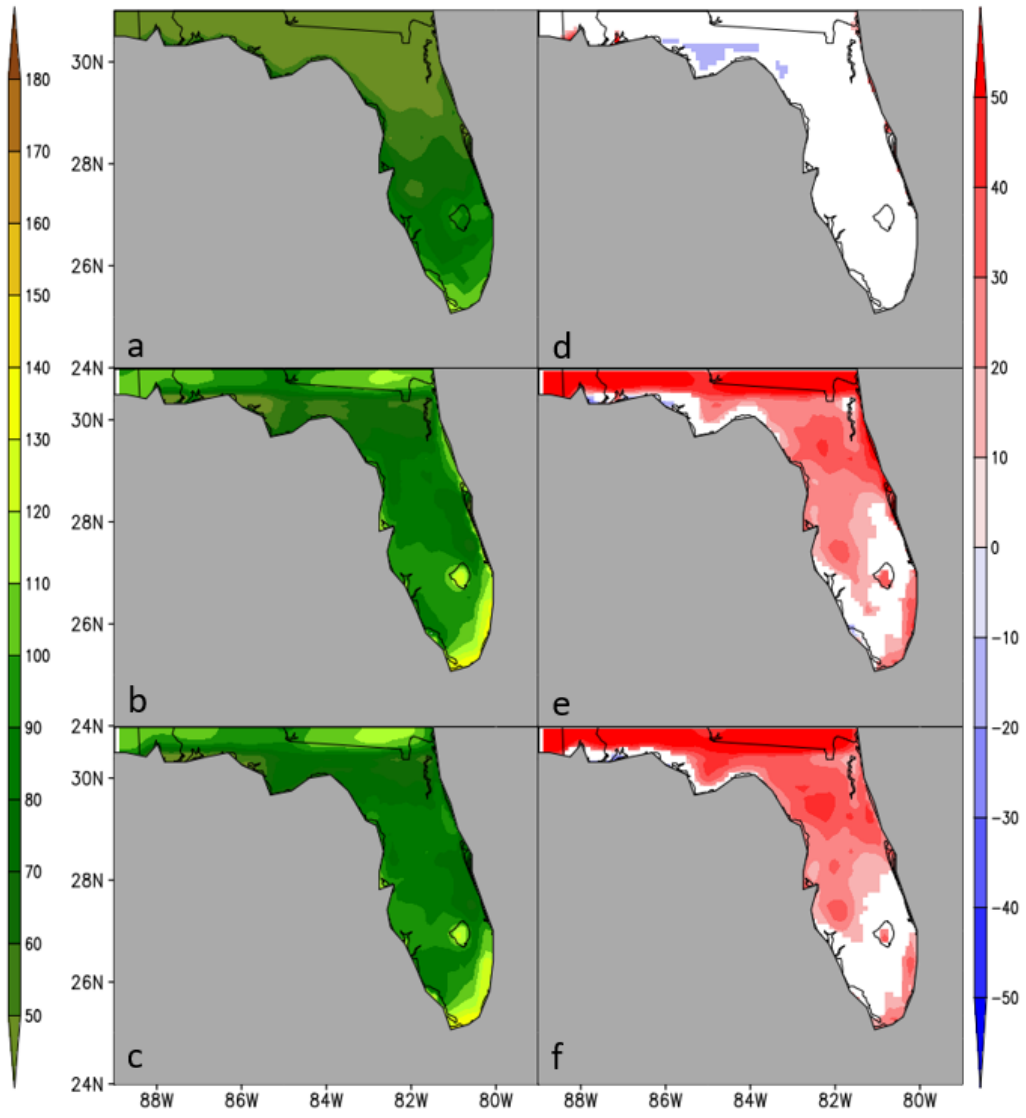

Fig. 3: The climatological number of 2-day heatwave events (heat index 80+ °F) over Florida for 1986-2005 (a) ERA5, (b) URSM, (c) CRSM, and (d) c-b. The corresponding systematic errors of (e) URSM and (f) CRSM. The difference between model (d) URSM-CRSM and corresponding systematic errors of (e) URSM, (f) CRSM. The differences which are statistically significant at 95% confidence interval according to t-test are shaded values in panels d, e, and f.

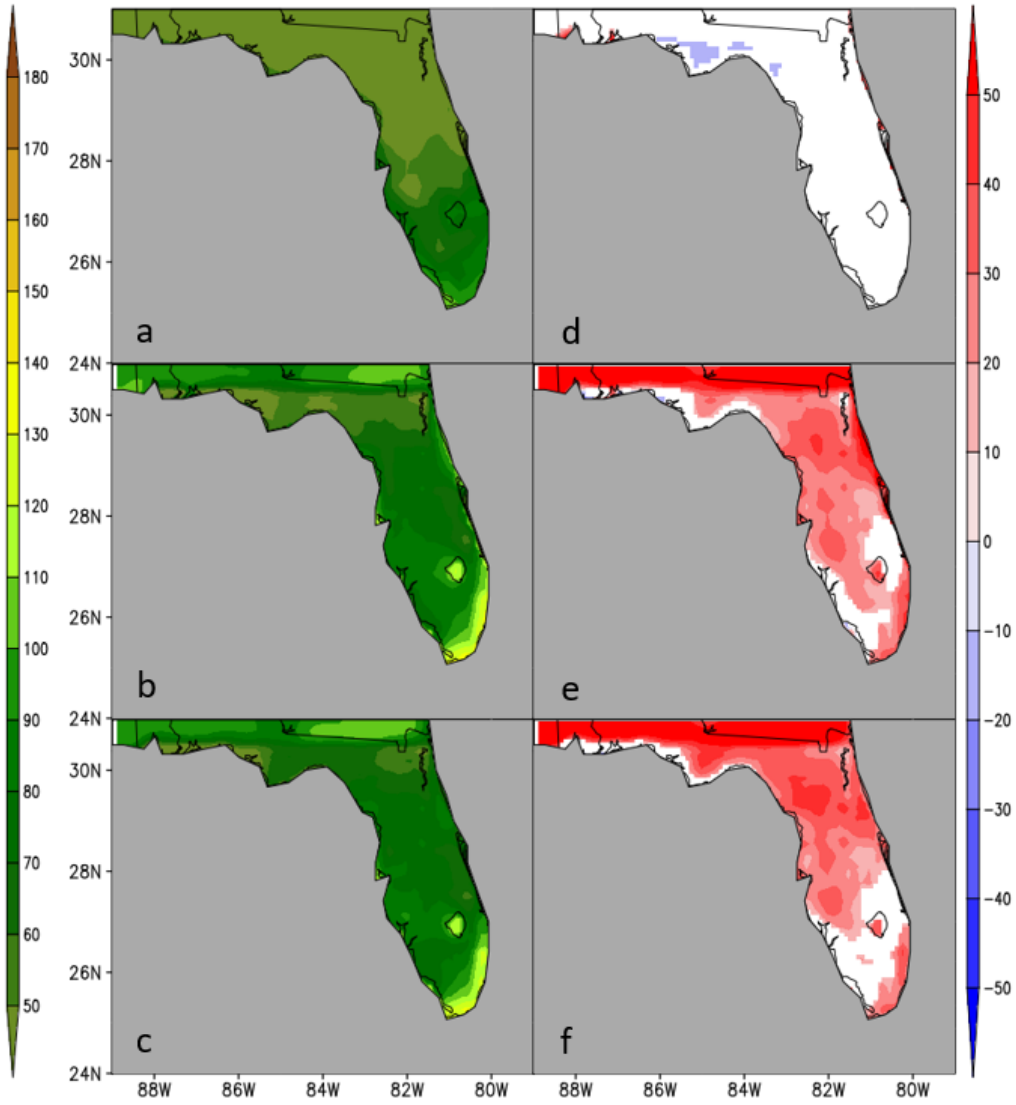

Fig. 4: The climatological number of 3-day heatwave events (heat index 80+ °F) over Florida for 1986-2005 (a) ERA5, (b) URSM, (c) CRSM, and (d) c-b. The corresponding systematic errors of (e) URSM and (f) CRSM. The difference between model (d) URSM-CRSM and corresponding systematic errors of (e) URSM, (f) CRSM. The differences which are statistically significant at 95% confidence interval according to t-test are shaded values in panels d, e, and f.

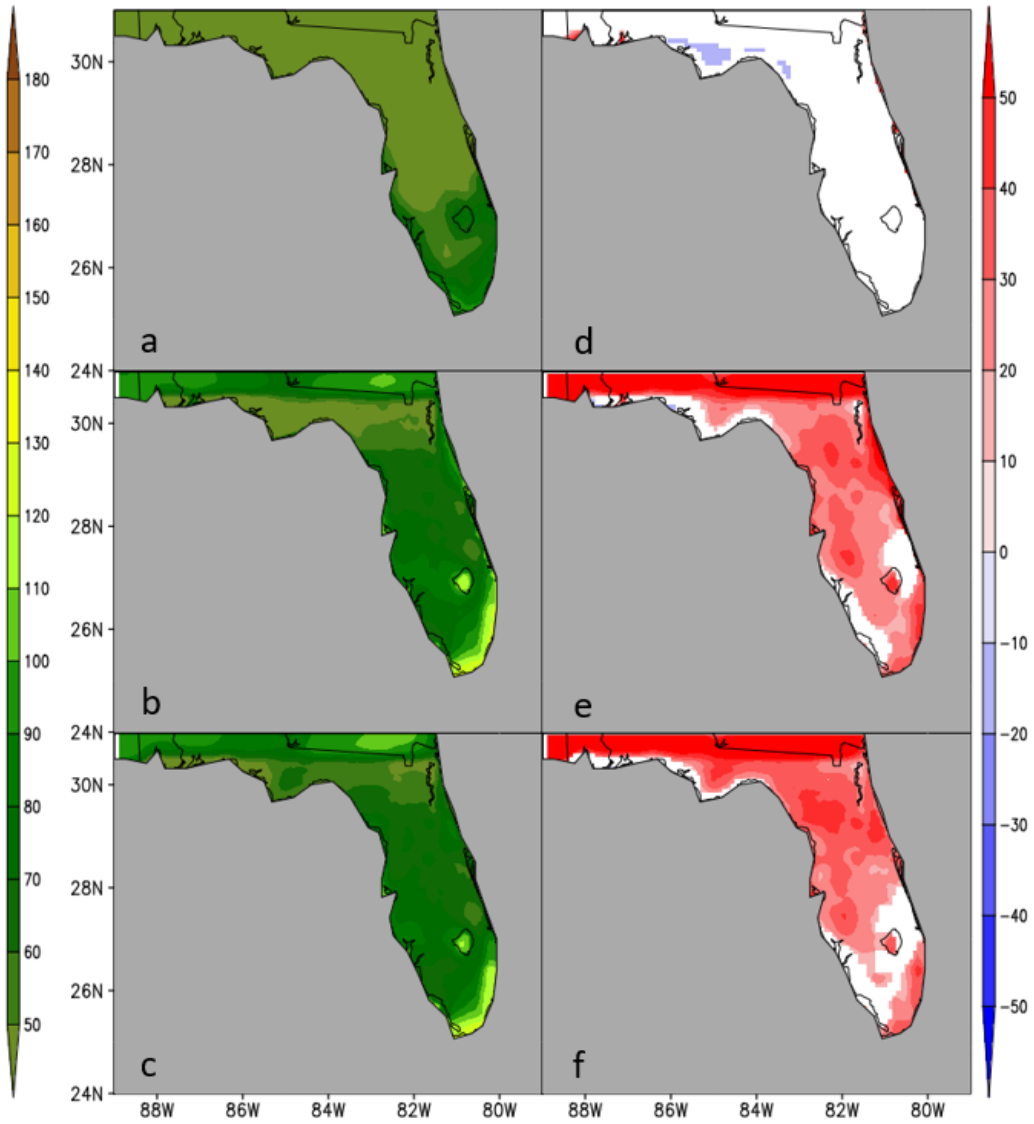

Fig. 5: The climatological number of 4-day heatwave events (heat index 80+ °F) over Florida for 1986-2005 (a) ERA5, (b) URSM, (c) CRSM, and (d) c-b. The corresponding systematic errors of (e) URSM and (f) CRSM. The difference between model (d) URSM-CRSM and corresponding systematic errors of (e) URSM, (f) CRSM. The differences which are statistically significant at 95% confidence interval according to t-test are shaded values in panels d, e, and f.

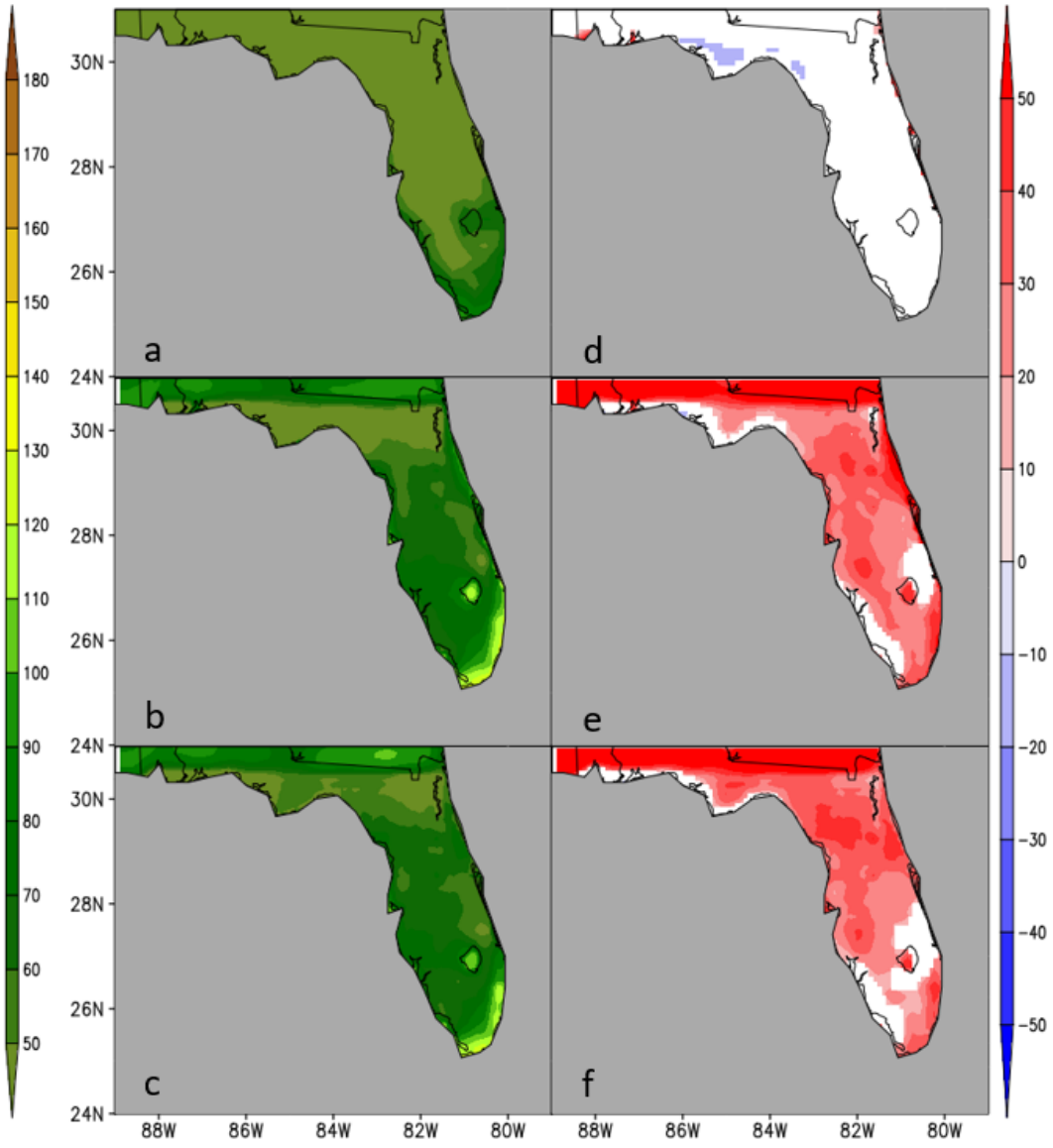

Fig. 6: The climatological number of 5-day heatwave events (heat index 80+ °F) over Florida for 1986-2005 (a) ERA5, (b) URSM, (c) CRSM, and (d) c-b. The corresponding systematic errors of (e) URSM and (f) CRSM. The difference between model (d) URSM-CRSM and corresponding systematic errors of (e) URSM, (f) CRSM. The differences which are statistically significant at 95% confidence interval according to t-test are shaded values in panels d, e, and f.

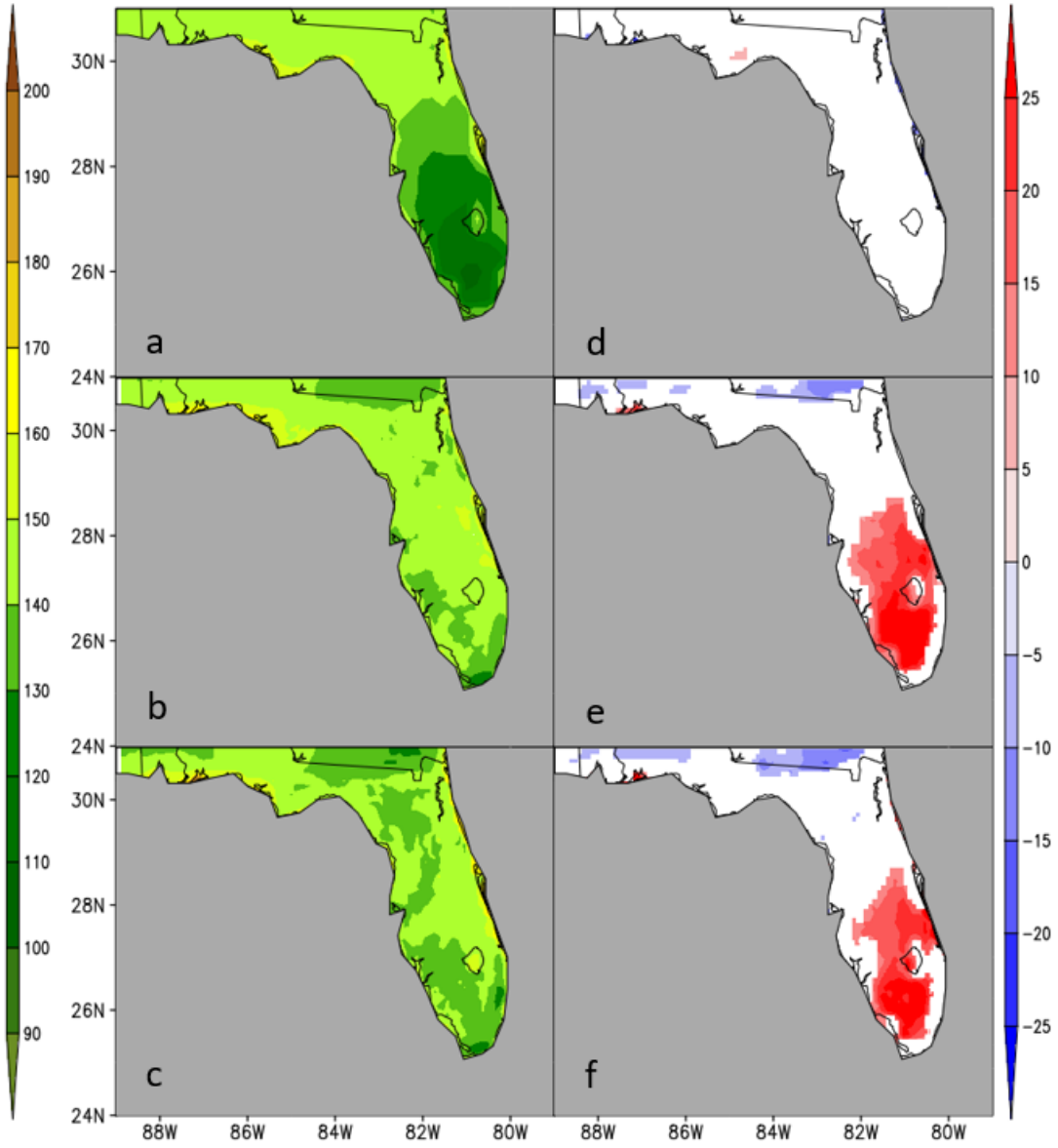

Fig. 7: The climatological first day of the year (in Julian day) for occurrence of the 1-day heatwave event for 1986-2005 from (a) ERA5, (b) URSM, (c) CRSM, and (d) c-b. The corresponding systematic errors from (e) URSM, and (f) CRSM. The differences which are statistically significant at 95% confidence interval according to t-test are shaded values in panels d, e, and f.

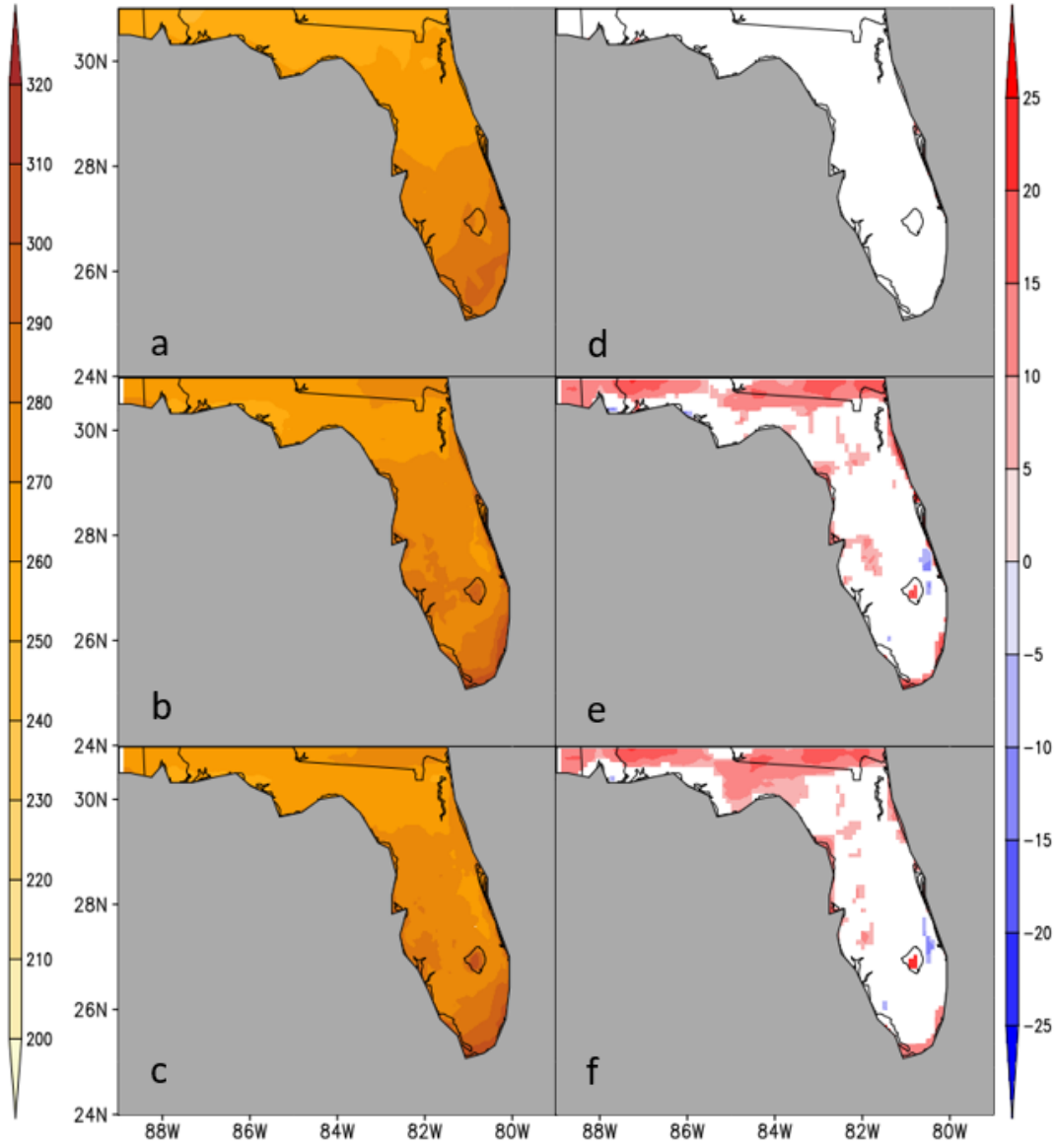

Fig. 8: The climatological last day of the year (in Julian day) for occurrence of the 1-day heatwave event for 1986-2005 from (a) ERA5, (b) URSM, (c) CRSM, and (d) c-b. The corresponding systematic errors from (e) URSM, and (f) CRSM. The differences which are statistically significant at 95% confidence interval according to t-test are shaded values in panels d, e, and f.

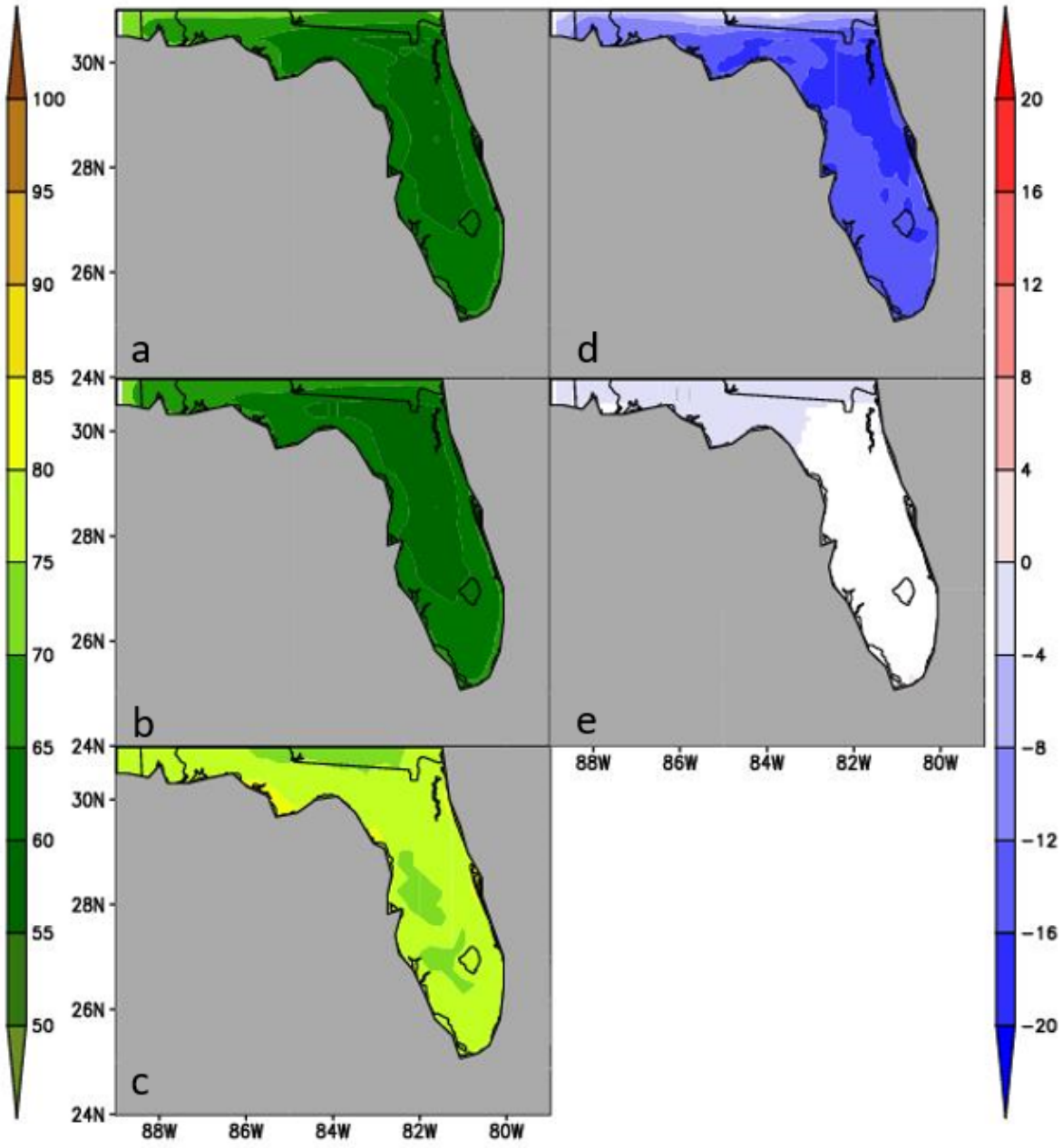

Fig. 9: The climatological 2 m relative humidity (%) associated with 1-day heatwave events from (a) URSM20, (b) URSM21, (c) ERA5, and (d) the corresponding systematic errors of URSM20 and (e) b-a..

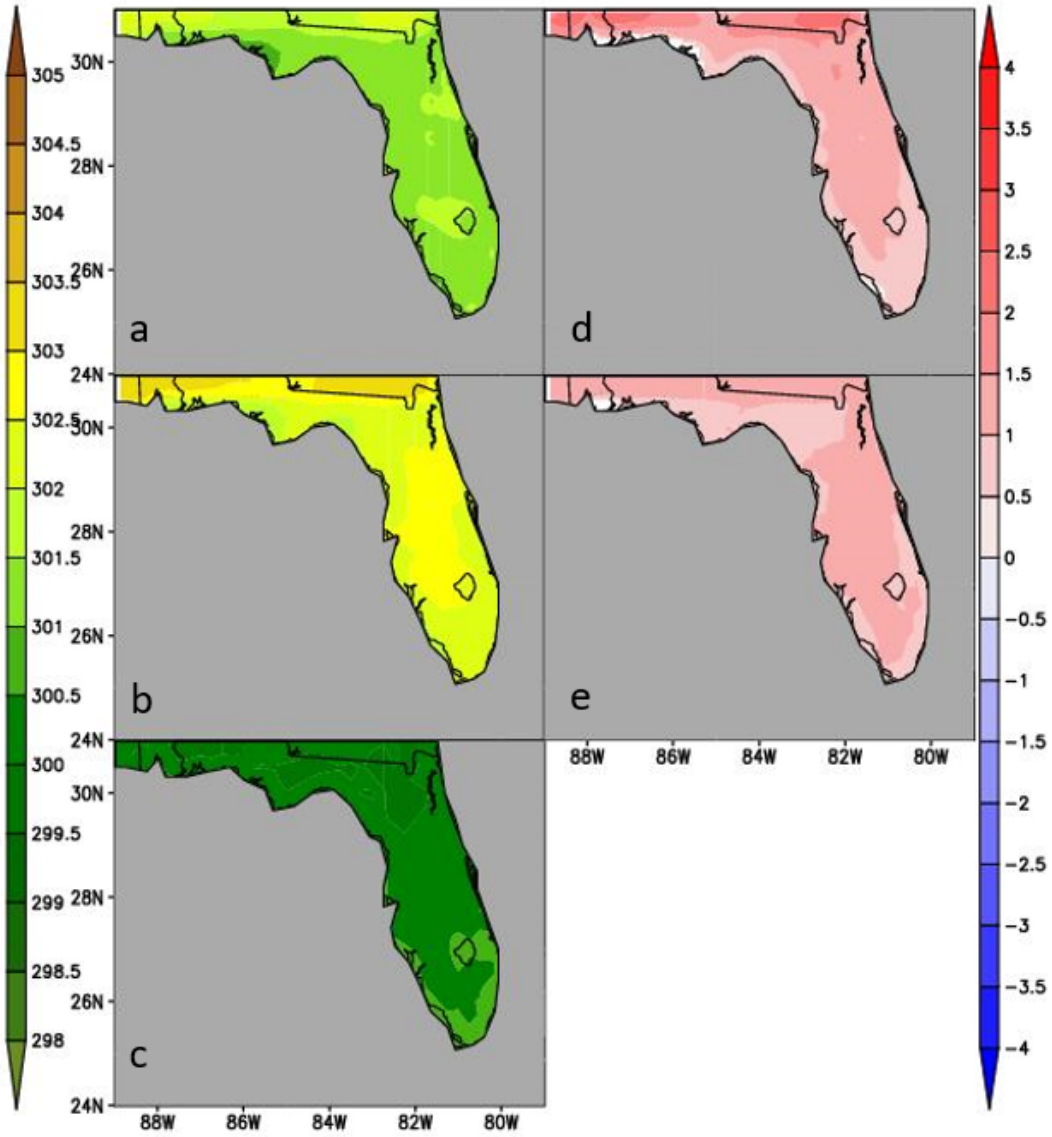

Fig. 10: The climatological 2 m air temperature (°K) associated with 1-day heatwave events from (a) URSM20, (b) URSM21, (c) ERA5, (d) the corresponding systematic errors of URSM20, and (e) b-a.

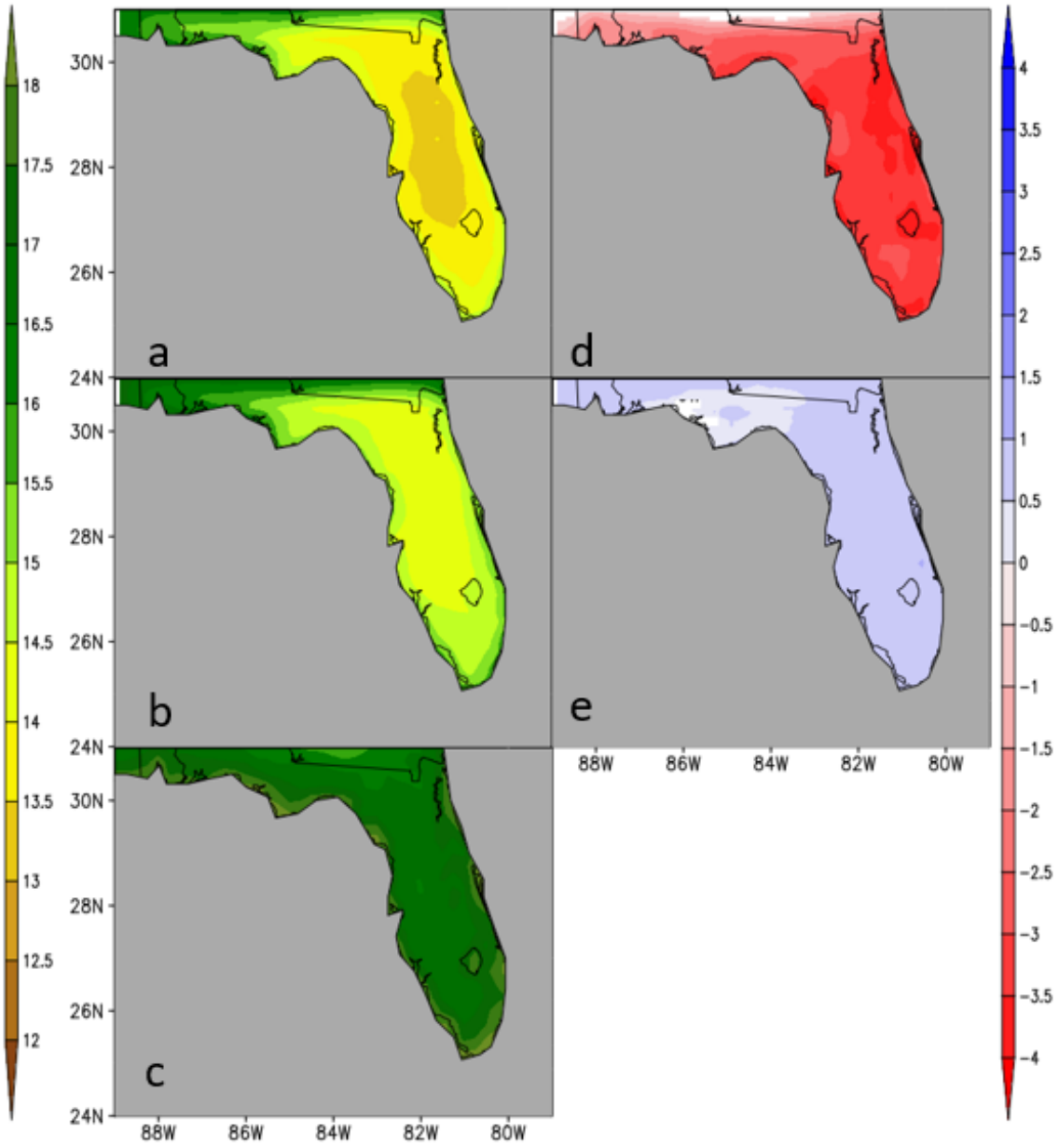

Fig. 11: The climatological 2 m specific humidity (kg/kg) associated with 1-day heatwave events from (a) URSM20, (b) URSM21, (c) ERA5, (d) the corresponding systematic errors of URSM20, and (e) b-a.

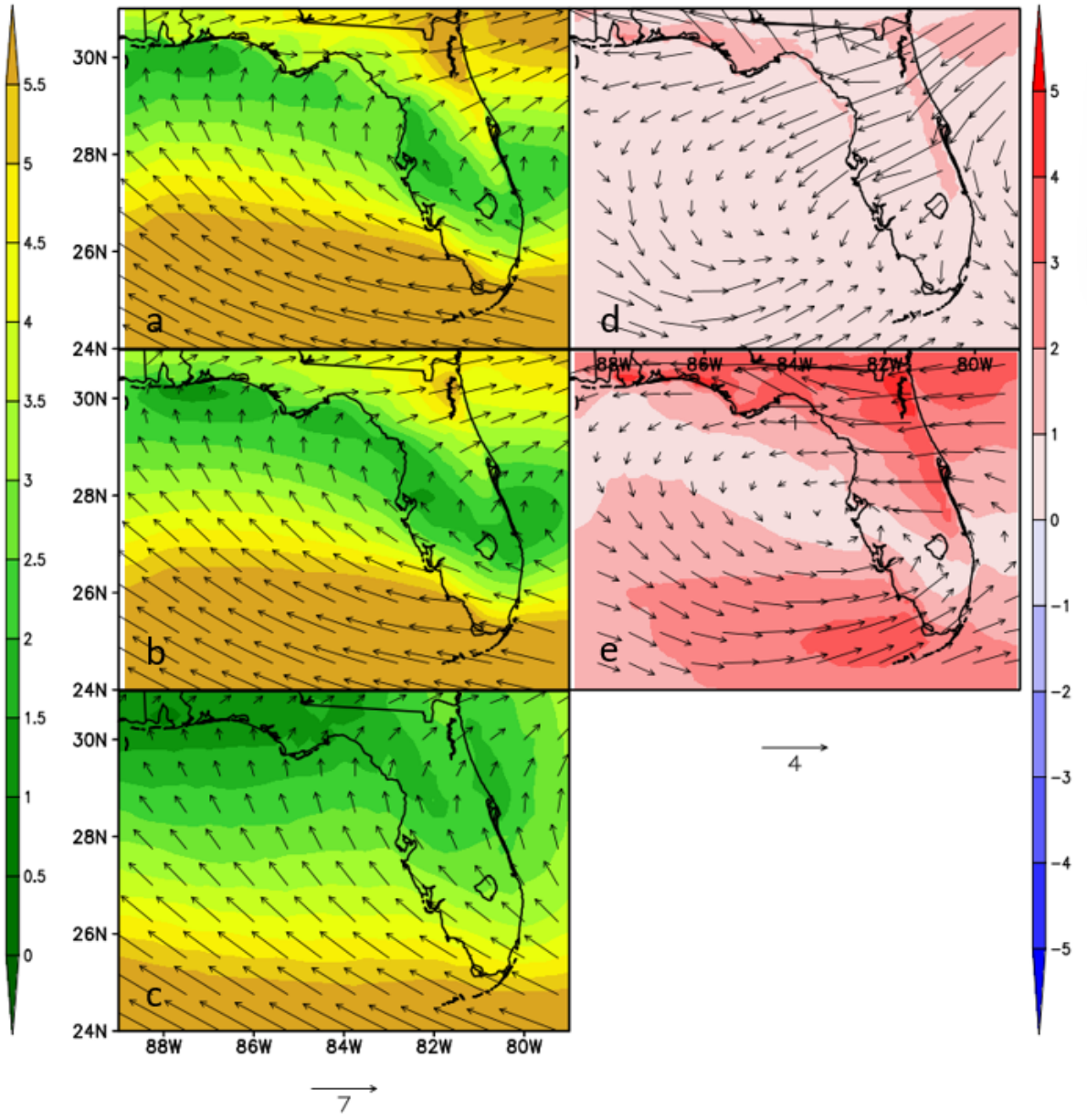

Fig. 12: The climatological 850hPa circulation and its magnitude (m/s; shaded) associated with 1-day heatwave events from (a) URSM20, (b) URSM21, (c) ERA5, (d) the corresponding systematic errors of URSM20, and (e) b-a.

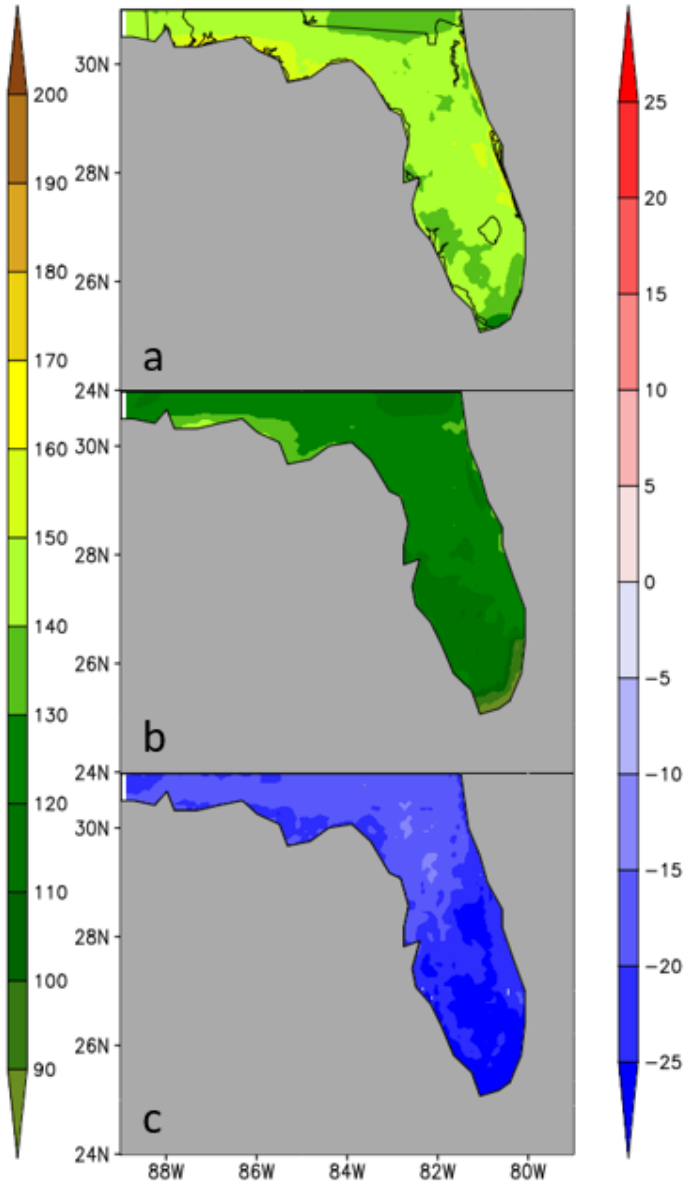

Fig. 13: The climatological first day of the year (in Julian day) for the occurrence of 1-day heatwave event from (a) URSM20, (b) URSM21, and (c) b-a.

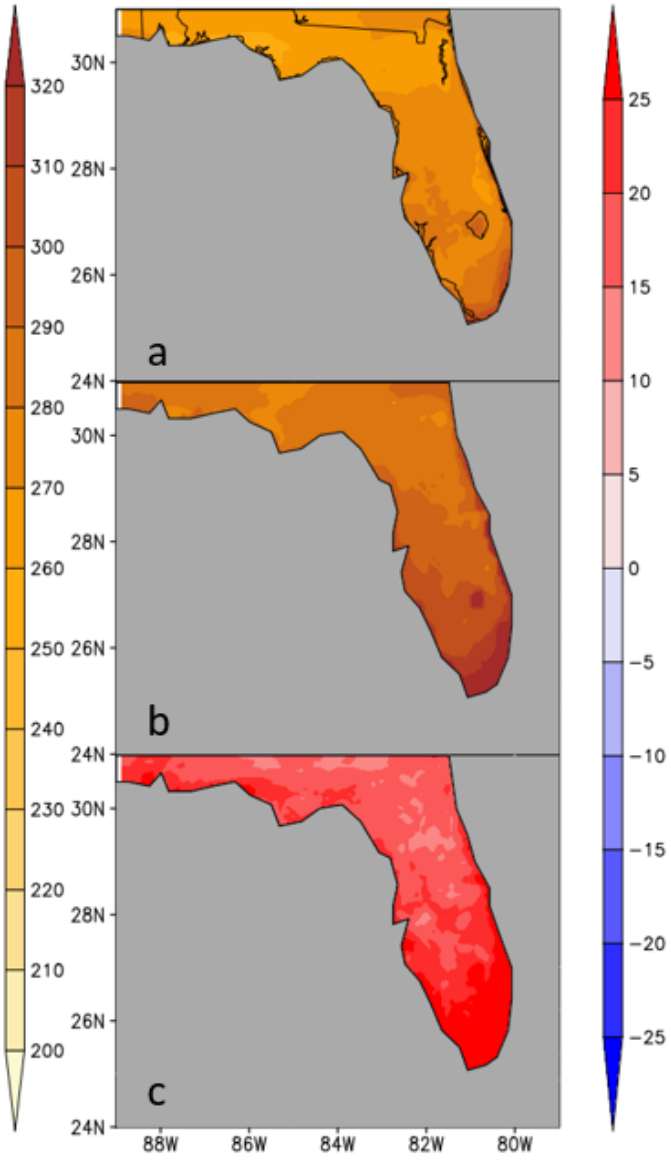

Fig. 14: The climatological last day of the year for the occurrence of 1-day heatwave event from (a) URSM20, (b) URSM21, and (c) b-a.

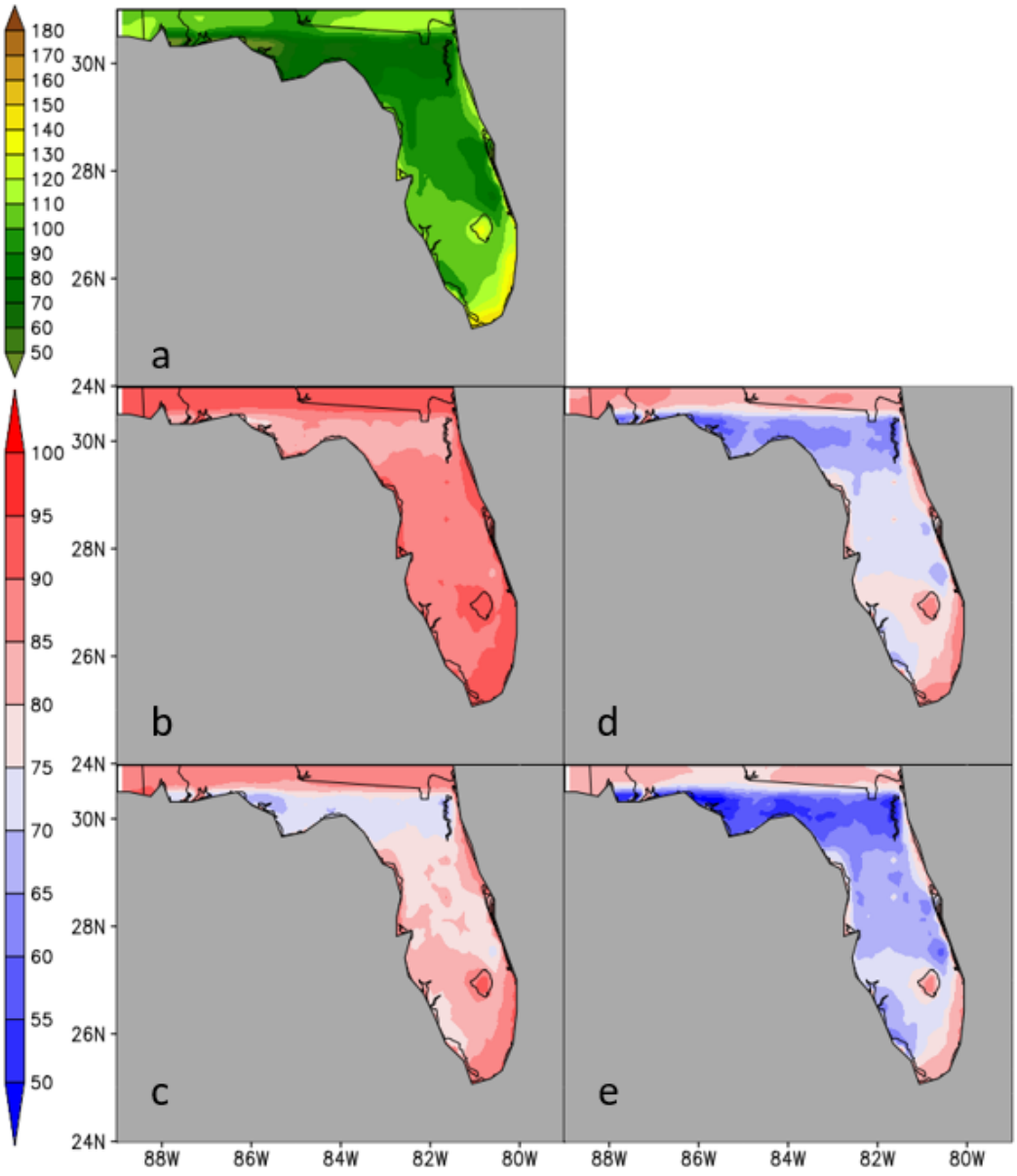

Fig. 15: (a) The climatological number of days of 1-day heatwave event from URSM20 for the period 1986-2005. The corresponding ratio of the climatological frequency of (b) 2-day, (c) 3-day, (d) 4-day, and (e) 5-day heatwave events to 1-day heatwave event from URSM20 simulation.

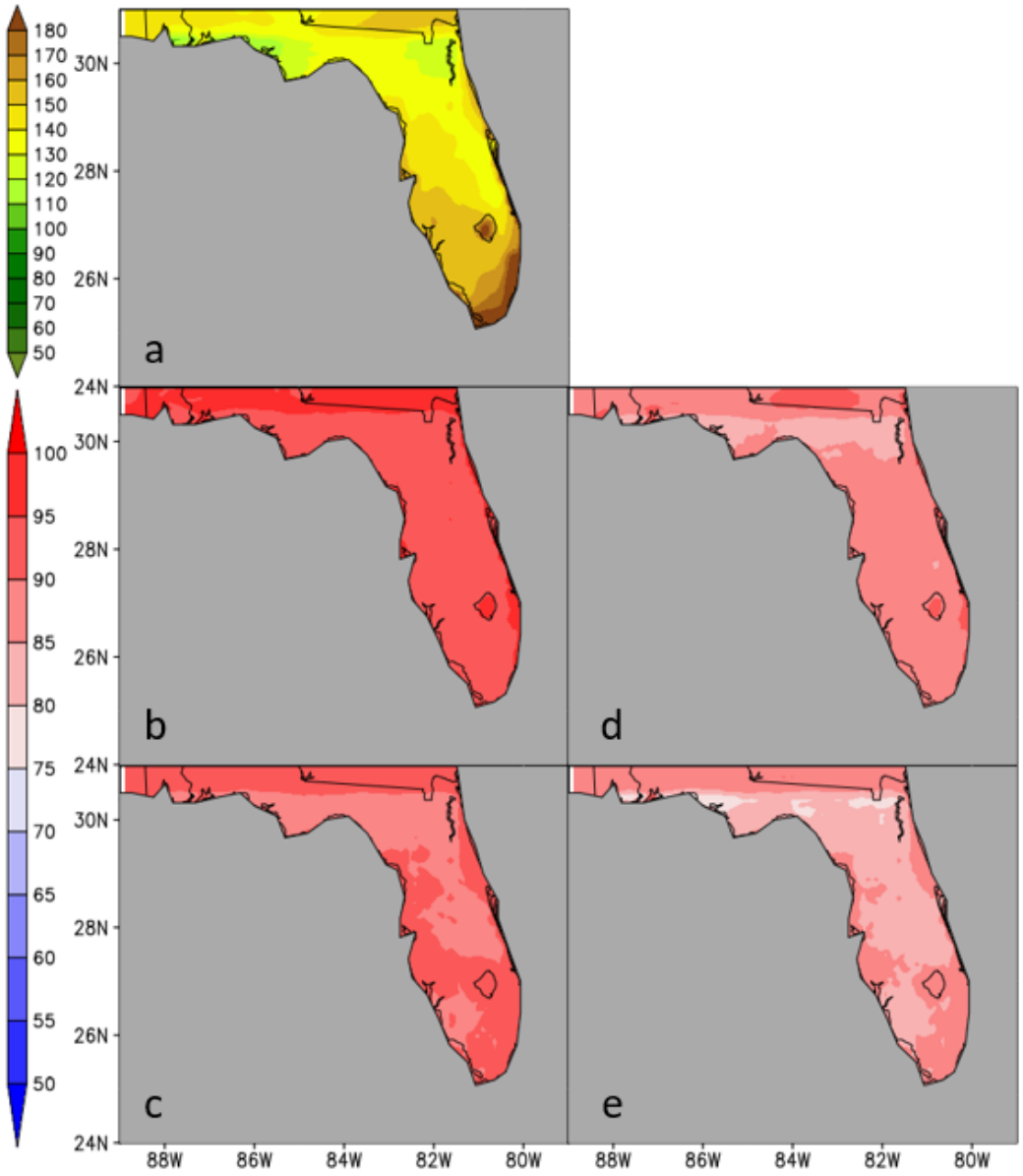

Fig. 16: (a) The climatological number of days of 1-day heatwave event from URSM21 for the period 2041-2060. The corresponding ratio of the climatological frequency of (b) 2-day, (c) 3-day, (d) 4-day, and (e) 5-day heatwave events to 1-day heatwave event from URSM21 simulation.

CHAPTER 5

CONCLUSION

This study was motivated to understand the future of heat waves in Florida. The study was conducted by analyzing the simulations from relatively high-resolution regional models rather than the coarser global models. This study first assessed the fidelity of the regional models by comparing their late 20th-century simulation to a reanalysis dataset, in terms of their intensity, duration, and seasonality. After this verification step, the regional model projection for the mid-21st century was analyzed. All terrestrial regions of Florida are impacted by heatwave events. Therefore, the assessment of the future heat waves in a warming climate will be critical for Florida's population, workforce, and environment.

In this study, we verified two regional climate models, one coupled to a regional ocean model (CRSM) and the other forced with prescribed SST (URSM) with respect to the ERA5 reanalysis dataset. Once the verification was performed, we used the projections of the mid-21st century climate from only the URSM to assess the heatwave events over Florida as we found the results in CRSM to be very similar. The regional spectral model (which is the atmospheric component of the regional climate model) is discretized at 10km grid spacing with the top at 2hPa. Both URSM and CRSM are forced at the atmospheric lateral boundary conditions at 6-hour intervals. The ocean in CRSM is forced at the lateral boundaries at monthly intervals. In comparison, the ERA5 dataset is available on a 31km grid.

For the late 20th century time period, the URSM and the CRSM verify reasonably well when compared to the reanalysis dataset. However, the model simulations display a systematic bias of overestimating the frequency of the heatwave events. This is associated with a dry and warm bias of surface humidity and surface temperature and the North Atlantic Subtropical High (NASH) being too far to the west.

The frequency of 1, 2, 3, 4, and 5-day heatwave events is overestimated in the URSM and CRSM. Furthermore, the climatological first day of the year for 1-day heatwave events occurs earlier in the reanalysis dataset for central and southern regions of Florida. The bias in the climatological last day of occurrence for 1-day heatwave events is comparatively much smaller. These systematic errors are associated with a warm and dry bias and a NASH that is displace further west than ERA5.

The future projections from URSM (URSM21) suggest an earlier and a later occurrence of the heatwave events for the year, thereby implying a long season for the likelihood of heatwave events. The URSM21 surface temperature projections indicate a general warming over all of Florida by 1-2°K. This projection is also accompanied by systematic drying of surface humidity in the mid-21st century climate. In addition, URSM21 indicates a weakening of the trade winds and the NASH.

The main caveat of this study is that the projections of the mid-21st century climate on the heat waves over Florida are made from a single 'imperfect' model. The upside however is that the projections are made at an unprecedented resolution of 10km grid spacing for Florida. This

horizontal resolution is important to resolve the vast coastlines of Florida that are otherwise misrepresented in many coarse global models (Misra et al. 2019; Narotsky and Misra 2022). Furthermore, the uncertainty of the model projections to natural variability and emission pathways is untested in this study. In addition, the uncertainty in changes to the seasonality of heatwaves over Florida in a future climate is not included in this work, however, we do analyze the start and end of the season because we choose to examine only HI13. Given HI13 is a low threshold for a heatwave, additional information about the severity of heatwaves in a future climate that exceed a higher threshold, such as HI14 (>90°F) or even HI15 (>105°F), has to be addressed in future studies.

REFERENCES

Androulidakis Y. S., Kourafalou V. Marine Heat Waves over Natural and Urban Coastal Environments of South Florida. Water. 2022; 14(23):3840. https://doi.org/10.3390/w14233840

Behrens, E., Fernandez, D., Sutton, P., Meridional Oceanic Heat Transport Influences Marine Heatwaves in the Tasman Sea on Interannual to Decadal Timescales, Frontiers in Marine Science, Vol. 6, 2019, https://www.frontiersin.org/articles/10.3389/fmars.2019.00228, DOI 10.3389/fmars.2019.00228, ISSN 2296-7745

Bhardwaj, A., and V. Misra, 2019: The role of air-sea coupling in the downscaled hydroclimate projection over Peninsular Florida and the West Florida Shelf Clim.
Dyn., https://doi.org/10.1007/s00382-019-04669-S.

Cloutier-Bisbee, Shealynn R., Ajay Raghavendra, and Shawn M. Milrad. "Heat Waves in Florida: Climatology, Trends, and Related Precipitation Events". Journal of Applied Meteorology and Climatology 58.3 (2019): 447-466. < https://doi.org/10.1175/JAMC-D-18-0165.1>. Web. 19 Jan. 2023.

Curran, E. Brian, Ronald L. Holle, and Raúl E. López. "Lightning Casualties and Damages in the United States from 1959 to 1994". Journal of Climate 13.19 (2000): 3448-3464. < https://doi.org/10.1175/1520-0442(2000)013<3448:LCADIT>2.0.CO;2>. Web. 21 Jan. 2023.

Dirmeyer, P. A., Balsamo, G., Blyth, E. M., Morrison, R., & Cooper, H. M. (2021). Land-atmosphere interactions exacerbated the drought and heatwave over northern Europe during summer 2018. AGU Advances, 2, e2020AV000283. https://doi.org/10.1029/2020AV000283

EPA 430-F-16-011., 2016. https://www.epa.gov/sites/default/files/2016-08/documents/climate-change-fl.pdf

Fennessy, M. J., and J. L. Kinter, III. "Climatic Feedbacks during the 2003 European Heat Wave". Journal of Climate 24.23 (2011): 5953-5967.
< https://doi.org/10.1175/2011JCLI3523.1>. Web. 10 Jan. 2023.

Florida Tax Watch. Aging in Place – The economic and Fiscal Value of Home and Community-Based Services. 2022. https://floridataxwatch.org/Research/Full-Library/aging-in-placethe-economic-and-fiscal-value-of-home-and-community-based-services#:~:text=Similar%20to%20demographic%20trends%20across,to%206.7%20million%20elderly%20residents

Gent, P.R., Danabasoglu, G., Denner, L.J., Holland, M.M., Hunke, E.C., Jayne, S.R., Lawrence, D.M., Neale, R.B., Rasch, P.J., Vertenstein, M., Worley, P.H., 2011. The community climate system model version 4. J. Clim. 24 (19), 4973-4991.

Guirguis Kristen, Alexander Gershunov, Alexander Tardy, and Rupa Basu. "The Impact of Recent Heat Waves on Human Health in California". Journal of Applied Meteorology and Climatology 53.1 (2014): 3-19. < https://doi.org/10.1175/JAMC-D-13-0130.1>. Web. 10 Jan. 2023.

Hersbach, H., Bell, W., Berrisford, P., Horanyi, A., Sabater, J. M., Nicolas, J., et al. (2019). The ERA5 global reanalysis. Quarterly Journal of the Royal Meteorological Society, 146, 1999–2049. https://doi.org/10.1002/qj.3803

Higgins, R. W., Y. Chen, and A. V. Douglas. "Interannual Variability of the North American Warm Season Precipitation Regime". Journal of Climate 12.3 (1999): 653-680. < https://doi.org/10.1175/1520-

Juang, H. H., and M. Kanamitsu, 1994: The NMC Nested Regional Spectral Model. Mon. Wea. Rev., 122, 3–26, https://doi.org/10.1175/1520-0493(1994)122<0003:TNNRSM>2.0.CO;2.

Keellings D., Waylen, P., Increased risk of heat waves in Florida: Characterizing changes in bivariate heat wave risk using extreme value analysis, Applied Geography, Volume 46, 2014, Pages 90-97, ISSN 0143-6228, https://doi.org/10.1016/j.apgeog.2013.11.008.

Klotzbach, P. J., Bowen, S. G., Pielke, R., Jr., & Bell, M. (2018). Continental U.S. Hurricane Landfall Frequency and Associated Damage: Observations and Future Risks, Bulletin of the American Meteorological Society, 99(7), 1359-1376. Retrieved Jan 9, 2023, from https://journals.ametsoc.org/view/journals/bams/99/7/bams-d-17-0184.1.xml

Li, X. Heat wave trends in Southeast Asia during 1979–2018: The impact of humidity. Science of The Total Environment. Volume 721. 2020. 137664. ISSN 0048-9697. https://doi.org/10.1016/j.scitotenv.2020.137664.

Li, N., Xiao, Z., and Zhao, L. "A Recent Increase in Long-Lived Heatwaves in China under the Joint Influence of South Asia and Western North Pacific Subtropical Highs". Journal of Climate 34.17 (2021): 7167-7179. < https://doi.org/10.1175/JCLI-D-21-0014.1>. Web. 10 Jan. 2023.

Liu, X., Guo, L., Huang, L., Chen, D. (2020). Similarities and Differences in the Mechanisms Causing the European Summer Heatwaves in 2003, 2010, and 2018. AGU. https://doi.org/10.1029/2019EF001386

Miller, A.J., Arias, M.E. & Alvarez, S. Built environment and agricultural value at risk from Hurricane Irma flooding in Florida (USA). Nat Hazards 109, 1327–1348 (2021). https://doi.org/10.1007/s11069-021-04880-w

Misra, V., 2020: Regionalizing Global Climate Variations: A Study of the Southeastern US Regional Climate.Elsevier, 324 pp, ISBN:978-0-12-821826-6.

Misra, V., Bhardwaj, A. Understanding the seasonal variations of Peninsular Florida. Clim Dyn 54, 1873–1885 (2020). https://doi.org/10.1007/s00382-019-05091-7

Misra, V., and A. Bhardwaj 2021: Estimating the thermodynamic and dynamic contributions to hydroclimatic change over Peninsular Florida J. Hydromet., https://doi.org/10.1175/JHM-D-20-0159.1

Misra, V., and A. Bhardwaj, 2022: The impact of air-sea coupling on the simulation of the hydroclimatic change over Peninsular Florida Clim. Dyn., https://doi.org/10.1007/s00382-022-06294-1.

Misra, V., and A. Mishra, 2016: The oceanic influence on the rainy season of Peninsular Florida. J. Geophys. Res. Atmos., 121, 7691–7709, https://doi.org/10.1002/2016JD024824

Misra, V., Bhardwaj, A., and Mishra, A. (2018). Characterizing the rainy season of Peninsular Florida. Clim. Dyn. 51, 2157–2167. doi: 10.1007/s00382-017- 4005-2

Misra, V., A. Mishra, and A. Bhardwaj, 2019: A coupled ocean-atmosphere downscaled climate projection for the peninsular Florida region. J. Mar. Syst., 194, 25–40, https://doi.org/10.1016/j.jmarsys.2019.02.010.

Misra, V., C B Jayasankar., Mishra, A., Mitra, A., Murugavel, P. 2022. Datasets from Regional Coupled Ocean-Atmosphere Model (RSM-ROMS) over South Asia. *Florida State University.* DOI 10.17605/OSF.IO/2YK64

Mix, Jacqueline., Elon, Lisa., Vi Thien Mac, Valerie., Flocks, Joan., Economos, Eugenia., Tovar-Aguilar, Antonio J., Stover Hertzberg., Vicki., McCauley, Linda A. Hydration Status, Kidney Function, and Kidney Injury in Florida Agricultural Workers. Journal of Occupational and Environmental Medicine, Volume 60, Number 5, 1 May 2018, pp. e253-e260(8). https://doi.org/10.1097/JOM.0000000000001261

Morano L.H., Watkins S., Kintziger K. A Comprehensive Evaluation of the Burden of Heat-Related Illness and Death within the Florida Population. International Journal of Environmental Research and Public Health. 2016; 13(6):551. https://doi.org/10.3390/ijerph13060551

Mukherjee, S., Mishra, A. K. (2020). Increase in Compound Drought and Heatwaves in a Warming World. AGU, Geophysical Research Letters. https://doi.org/10.1029/2020GL090617

Narotsky, C. D. and V. Misra 2022: The Seasonal Predictability of the Wet Season over Peninsular Florida Int. J. Climatol., https://doi.org/10.1002/joc.7423

National Drought Mitigation Center, University of Nebraska-Lincoln. Drought monitor; Florida. 2023. https://droughtmonitor.unl.edu/CurrentMap/StateDroughtMonitor.aspx?FL

NOAA office for coastal management. Hurricane Costs. 2023. https://coast.noaa.gov/states/fast-facts/hurricane-costs.html

Noska, R., and V. Misra (2016), Characterizing the onset and demise of the Indian summer monsoon, Geophys. Res. Lett., 43, 4547–4554, doi:10.1002/ 2016GL068409.

NWS.a NOAA. https://www.weather.gov/safety/heat-during#:~:text=What%20is%20a%20heat%20wave,of%20people%20to%20hazardous%20heat.

NWS.b NOAA. https://www.weather.gov/cae/lightningdeaths.html

Perkins, S. E., L. V. Alexander, and J. R. Nairn, 2012: Increasing frequency, intensity and duration of observed global heatwaves and warm spells. Geophys. Res. Lett., 39, L20714, https://doi.org/10.1029/2012GL053361.

Raghavendra, A., Dai, A., Milrad, S.M. et al. Floridian heatwaves and extreme precipitation: future climate projections. Clim Dyn 52, 495–508 (2019). https://doi.org/10.1007/s00382-018-4148-9

Rameezdeen R, Elmualim A. The Impact of Heat Waves on Occurrence and Severity of Construction Accidents. International Journal of Environmental Research and Public Health. 2017; 14(1):70. https://doi.org/10.3390/ijerph14010070

Russo, E. and Domeisen, D.: A global comparison of heatwave magnitude indices using ERA5 reanalysis data, EMS Annual Meeting 2022, Bonn, Germany, 5–9 Sep 2022, EMS2022-176, https://doi.org/10.5194/ems2022-176, 2022.

Sánchez-Benítez, Antonio, Helge Goessling, Felix Pithan, Tido Semmler, and Thomas Jung. "The July 2019 European Heat Wave in a Warmer Climate: Storyline Scenarios with a Coupled Model Using Spectral Nudging". Journal of Climate 35.8 (2022): 2373-2390. < https://doi.org/10.1175/JCLI-D-21-0573.1>. Web. 10 Jan. 2023.

Schär, C., Vidale, P., Lüthi, D. et al. The role of increasing temperature variability in European summer heatwaves. Nature 427, 332–336 (2004). https://doi.org/10.1038/nature02300

Schoof, J. T., T. W. Ford, and S. C. Pryor. "Recent Changes in U.S. Regional Heat Wave Characteristics in Observations and Reanalyses". Journal of Applied Meteorology and

Climatology 56.9 (2017): 2621-2636. < https://doi.org/10.1175/JAMC-D-16-0393.1>. Web. 18 Jan. 2023.

Sheridan, S. C., and C. C. Lee, 2018. Temporal trends in absolute and relative extreme temperature events across North America. J. Geophys. Res. Atmos., 123, 11 889–11 898, https://doi.org/10.1029/2018JD029150.

Semenza C. Jan, Ph.D., M.P.H., Rubin H. Carol, D.V.M., M.P.H., Falter H. Kenneth, Ph.D., Selanikio D. Joel, M.D., W. Dana Flanders, M.D., D.Sc., Howe L. Holly, Ph.D., and Wilhelm L. John, M.D., M.P.H., 1996. Heat-Related Deaths during the July 1995 Heat Wave in Chicago. *The new England Journal of Medicine.* https://www.nejm.org/doi/full/10.1056/NEJM199607113350203

Sittel, M. C., 1994., Marginal probabilities of the extremes of ENSO events for temperature and precipitation in the southeastern United States. Tech. Rep. 94-1, Center for Ocean–Atmospheric Studies, The Florida State University, Tallahassee, FL

Smith, T.T., Zaitchik, B.F., Gohlke, J.M., 2013. Heat waves in the United States: definitions, patterns, and trends. Clim. Change 118, 811–825. doi: 10.1007/s10584-012-0659-2.

Sparks, J., Changnon, D., & Starke, J. (2002)., Changes in the Frequency of Extreme Warm-Season Surface Dewpoints in Northeastern Illinois: Implications for Cooling-System Design and Operation, Journal of Applied Meteorology, 41(8), 890-898. Retrieved Jan 7, 2023, from https://journals.ametsoc.org/view/journals/apme/41/8/1520-0450_2002_041_0890_citfoe_2.0.co_2.xml

Thapa, B., Cahyanto, I., Holland, S. M., Absher, J. D., Wildfires and tourist behaviors in Florida, Tourism Management, Volume 36, 2013, Pages 284-292, ISSN 0261-5177, https://doi.org/10.1016/j.tourman.2012.10.011.

Thomas, Natalie P., Michael G. Bosilovich, Allison B. Marquardt Collow, Randal D. Koster, Siegfried D. Schubert, Amin Dezfuli, and Sarith P. Mahanama. "Mechanisms Associated with Daytime and Nighttime Heat Waves over the Contiguous United States". Journal of Applied Meteorology and Climatology 59.11 (2020): 1865-1882. < https://doi.org/10.1175/JAMC-D-20-0053.1>. Web. 10 Jan. 2023.

Shimon Wdowinski, Ronald Bray, Ben P. Kirtman, Zhaohua Wu. 2016. Increasing flooding hazard in coastal communities due to rising sea level: Case study of Miami Beach, Florida., Ocean & Coastal Management., Volume 126., Pages 1-8, ., ISSN 0964-5691., https://doi.org/10.1016/j.ocecoaman.2016.03.002.

Wu, J., Zhou Y., Gao Y., Joshua S. Fu., B. A., Huang, C., Kim, Y., and Liu, Y. 2014. Estimation and Uncertainty Analysis of Impacts of Future Heat Waves on Mortality in the Eastern United States. Environmental Health Perspectives. https://doi.org/10.1289/ehp.1306670

Zhang Y, Mao G, Chen C, Shen L, Xiao B. Population Exposure to Compound Droughts and Heatwaves in the Observations and ERA5 Reanalysis Data in the Gan River Basin, China. Land. 2021; 10(10):1021. https://doi.org/10.3390/land10101021

BIOGRAPHICAL SKETCH

Parker Beasley was born and raised in Orlando, FL in 1998. In August of 2004 he realized his passion for meteorology when Hurricane Charlie struck his hometown. In high school, Parker applied to Florida State University and was accepted. He started his academic career at FSU in the Fall of 2017. During his time as an undergraduate, Parker took up broadcast meteorology and had an internship in the Summer of 2019 in Orlando, FL at one of the stations he grew up watching. During his senior year he would become a freelance broadcast meteorologist in Columbus, GA. He would also begin to work with Dr. Misra on his undergraduate thesis that has since been published. Upon completion of his Bachelor of Science in Meteorology he enrolled in graduate school at Florida State University and continued to work with Dr. Misra. With the submission of this thesis, Parker will graduate with a M.S. in Meteorology in the Spring of 2023. After graduating, he plans to apply his education, skills, and experience to the field of Meteorology.